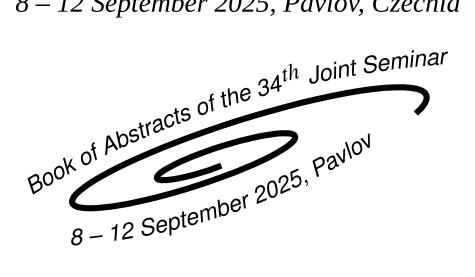
DMSRE 2025

Development of Materials Science in Research and Education

8 – 12 September 2025, Pavlov, Czechia





Organized by

Czechoslovak Association for Crystal Growth Slovak Expert Group of Solid State Chemistry and Physics

Under the auspicies of

Institute of Physics of the Czech Academy of Sciences Slovak Society for Industrial Chemistry Faculty of Chemical and Food Technology STU in Bratislava Faculty of Materials Science and Technology STU in Trnava

Development of Materials Science in Research and Education

8 – 12 September 2025, Pavlov, Czechia

Book of Abstracts of the 34th Joint Seminar

Topics

- Trends in development of materials research
- Information about the research programs of individual institutions
- · Results of materials research
- Education of materials science at the universities
- Information about equipment for preparation and characterisation of materials





Scientific Committee

Chair: Mária Behúlová (Faculty of Material Science and Technology SUT, Trnava)

Co-chair: Zdeněk Kožíšek (Institute of Physics of the Czech Academy of Sciences, Prague)

Monika Losertová (Technical University of Ostrava, Ostrava)

Jan Grym (Institute of Photonics and Electronics, Prague)

Vladimír Kuchtanin (Slovak University of Technology in Bratislava, Bratislava)

Maroš Martinkovič (Faculty of Material Science and Technology SUT, Trnava)

Petr Mošner (University of Pardubice, Pardubice)

Jan Polák (Crytur Turnov, Turnov)

Zdeněk Potůček (Faculty of Nuclear Sciences and Physical Engineering CTU, Prague)

Kateřina Rubešová (University of Chemistry and Technology, Prague)

Organizing Committee

Chair: Robert Král (Institute of Physics of the Czech Academy of Sciences, Prague)

Mária Behúlová (Faculty of Material Science and Technology SUT, Trnava)

Aleš Bystřický (Institute of Physics of the Czech Academy of Sciences, Prague)

Vítězslav Jarý (Institute of Physics of the Czech Academy of Sciences, Prague)

Herbert Kindl (Institute of Physics of the Czech Academy of Sciences, Prague)

Zdeněk Kožíšek (Institute of Physics of the Czech Academy of Sciences, Prague)

Kateřina Křehlíková (Institute of Physics of the Czech Academy of Sciences, Prague)

Zdeňka Poláčková (Institute of Physics of the Czech Academy of Sciences, Prague)

Vojtěch Vaněček (Institute of Physics of the Czech Academy of Sciences, Prague)

Petra Zemenová (Institute of Physics of the Czech Academy of Sciences, Prague)

Supported by the Czechoslovak Association for Crystal Growth (CSACG) CZ-162 00 Prague 6, Cukrovarnická 10, Czech Republic

Published by the Institute of Physics of the Czech Academy of Sciences, v. v. i. CZ-182 21 Prague 8, Na Slovance 1999/2, Czech Republic

Editors: Zdeněk Kožíšek, Robert Král, and Petra Zemenová

ISBN 978-80-909577-0-1



PREFACE

The 34th Joint Seminar "Development of Materials Science in Research and Education" (DMSRE34) will be held on 8 – 12 September 2025, in hotel IRIS Pavlov. The first Joint Seminar in these series was held at Gabčíkovo in Czechoslovakia in 1991. Seminar is organized by the Czechoslovak Association for Crystal Growth and the Slovak Expert Group of Solid State Chemistry and Physics under the auspicies of the Institute of Physics of the Czech Academy of Sciences, Faculty of Chemical and Food Technology SUT Bratislava, and Slovak Society for Industrial Chemistry every year with one break in 2021 (COVID-19 pandemic).

The Seminar brings together a unique combination of scientists across a multidisciplinary spectrum and provides an ideal forum for the presentations and discussions of recent developments and achievements in all theoretical and experimental aspects of preparation processes, characterization and applications of materials in bulk, thin film, nano-crystalline and glassy states.

The program will include 4 keynote lectures (35 minutes): ...

All other contributions will be presented as short lecture talks (20 minutes including discussion). The official languages of the seminar are English, Czech, and Slovak.

This booklet contains the abstracts of all contributions, which reached us before 16 August 2025. The authors are responsible for the technical and language quality of the contributions. The conference will run from Monday afternoon, 8 September 2025, untill Friday noon, 12 September 2025 in the hotel IRIS Pavlov, Czech Republic.

Dear colleagues, we welcome you to the 34^{th} DMSRE Joint Seminar and we hope you will enjoy your stay in Pavlov.

Zdeněk Kožíšek, Robert Král, and Petra Zemenová (Editors)

CONTENT

Program
Abstracts
Using Cayley graphs in costruction of large scale computer networks
Influence of Dual-Beam Laser Welding Parameters on the Geometry of a Duplex Stainless Steel Butt Welds: A Numerical Approach
Influence of argon shielding gas flow rate on the cooling and solidification of AA5087 aluminum alloy during wire arc additive manufacturing
Comparison of structural changes in SAC305 and SAC108 lead-free solders alloyed with gallium18 <u>Ivona Černičková</u> , Libor Ďuriška, Patrícia Danišovičová, Marián Drienovský, Terézia Machajdíková, Michaela Halmanová, and Roman Čička
Influence of Bi addition on microstructure and thermal properties of SAC108 solders
The determination of the material properties using DIC
Investigation of chemically induced degradation on the microstructure and morphology of Li-ion battery cathode
<u>Libor Ďuriška</u> , Ivona Černičková, Jakub Rafajdus, Martin Kusý, Marián Drienovský, Lenka Blinová, Santanu Mukherjee, and Jakub Reiter
Optimization of the 3D freeforming process of PIM feedstock in granular form
Crystallographic Orientation-Dependent Growth of Nanoparticles via Magnetron Sputtering on monocrystalline Rutile ${\rm TiO}_2$
Pushing limits of Mixed Glass Former Effect in Lithium Borophosphate glasses
Analysis of causes of cracking of piston rings mad of graphite cast iron
Where No One Else Dares: Growing Bulk Sulfide Single Crystals
Construction of Wannier orbitals and calculation of crystal field parameters of Ce-doped $Y_3Al_5O_{12}$ 27 <u>Jakub Ježek</u> and David Sedmidubský
Nonstandard use of powder diffraction methods for qualitative phase analysis

Influence of cutting edge microgeometry on the cutting forces and surface roughness of machining difficult-to- cut materials
František Jurina, Tomáš Vopát, Marek Vozár, Boris Pätoprstý, and Dominik Zajko
The melt growth of Al_2O_3 /YAG composite doped with cerium by Horizontal Directed crystalisation using Al_2O_3
seed30 Juraj Kajan, Tomáš Gregor, Anna Prnová, Peter Švančárek, Grigori Damazyan, Jakub Michalík, Mykhailo Chaika, and Dušan Galusek
Development of crucible free crystal growth technique for high melting temperature oxide materials 31 Kei Kamada
TESTOVACÍ TECHNIKA s.r.o company presentation
Monovalent ion doping effect on the scintillation properties of BaCl ₂ single crystals for eutectic type therma neutron detector
Ryosuke Kawabata, Masao Yoshino, Kei Kamada, Kyoung Jin Kim, Naoko Kutsuzawa, Rikito Murakami, Ak- ihiro Yamaji, Satoshi Ishizawa, Takashi Hanada, Yuui Yokota, Shunsuke Kurosawa, Hiroki Sato, and Akiro Yoshikawa
Development and characterization of nanoparticle-infused glass rods prepared via the micro-pulling-down
method
Analysis of the Laser Beam Trajectory and its Impact on the Cut in Material PMMA35 <u>Jana Knedlová,</u> Ondřej Bílek, Michal Hanus, and David Bartík
Analysis of welding simulation results using DOE methodology
Structure and properties of silver phosphate glasses with tungsten trioxide
A review of nucleation models in various systems
Laser performance overview of rare-earth doped multicomponent garnet crystal Gd ₃ (Ga,Al) ₅ O ₁₂ 39 <u>Jan Kratochvíl</u> , Pavel Boháček, Dominika Popelová, Jan Šulc, Michal Němec, Helena Jelínková, Bohumi Trunda, Lubomír Havlák, Karel Jurek, and Martin Nikl
Red-emitting ${ m Li}_2$ MnCl $_4$ for neutron detection: crystal growth and new doping strategies
Design and optimization of a rotating sample holder for high-temperature ion implantation
Statistical evaluation of metal plated polymer surfaces
Transparent Wood as a Sustainable Material for Photovoltaic Applications
Reliability of multi-state repairable systems44

Development and Application of HAXPES at TPS
Application of finite difference method in solving phase-field models
Evaluation of the Physico-Mechanical Properties of ABS Polymer for Automotive Applications 47 Lenka Markovičová, Viera Zatkalíková, and Milan Uhríčik
Influence of welding parameters on the microstructure and properties of laser welds of duplex steels 48 <u>Maroš Martinkovič</u> , Pavel Kovačócy, and Beáta Šimeková
Study of the effect of plate thickness on spatial resolution in novel optical guiding crystal scintillator49 <u>Yuhei Nakata</u> , Kei Kamada, Tetsuo Kudo, Masao Yoshino, Yasuyuki Usuki, Naveenkarthik Murugesan, Kyoung Jin Kim, Yuui Yokota, Syunsuke Kurosawa, Hiroki Sato, Takashi Hanada, Rikito Murakami, Akihiro Yamaji Satoshi Ishizawa, and Akira Yoshikawa
Drag finishing as a post-treatment process of increasing the cobalt content in cemented carbide after plasma polishing
Boris Pätoprstý, Tomáš Vopát, Martin Sahul, and Samuel Lenghart
Thermal Plasma for the Synthesis of Advanced Functional Nanomaterials51 <u>Jakub Pilař</u> , Alan Mašláni, and Maksym Buryi
Micro-pulling-down grown Tm,Ho:GSAG crystal as laser gain medium
Optical spectroscopy and surface properties of doped nanocrystalline ZnO thin films on interdigital electrodes
<u>Zdeněk Remeš</u> , Neda Neykova, Naini Jain, Rupendra Kumar Sharma, Jakub Holovský, Egor Ukraintsev Jaroslav Kuliček, Bohuslav Rezek, and Hua Shu Hsu
Plasmonic absorption in metal-ZnO nanocomplexes54 <u>Bohuslav Rezek</u> , Vendula Hrnčířová, Muhammad Qamar, and Egor Ukraintsev
Measurement of Thermally Induced Depolarization in Flash-lamp Pumped Nd:YAG Laser Rod55 <u>Adam Říha</u> , Helena Jelínková, Jan Šulc, David Vyhlídal, Karel Veselský, Kryštof Kadlec, and Karel Nejezchlel
Lutetium hafnates: From ceramics to OFZ-grown single crystals
Isotherm Study of Metribuzin and Tebuconazole Adsorption on Various Carbonaceous Materials57 <u>Margita Ščasná</u> , Alexandra Kucmanová, Maroš Sirotiak, Michal Hebnár, and Maroš Soldán
Comparative Study of Selected Decontamination Agents for Surface Decontamination of Radionuclides 58 <u>Margita Ščasná</u> , Maroš Sirotiak, Alexandra Kucmanová, Tatiana Valová, and Maroš Soldán
Structural, Morphological, and Optical Analysis of High-Purity ZnO Microrods59 Shelja Sharma and Maksym Buryi
Analysis of Wire Electrode Wear in the WEDM Machining of Inconel 625

Single Crystal Growth of Mg and Ce co-doped $Y_3(Ga,Al)_5O_{12}$ with various Mg concentration and their scintillation properties
<u>Hisato Suezumi</u> , Kei Kamada, Masao Yoshino, Kyoung Jin Kim, Rikito Murakami, Satoshi Ishizawa, Akihiro Yamaji, Shunsuke Kurosawa, Yuui Yokota, Hiroki Sato, Takashi Hanada, and Akira Yoshikawa
Temperature dependence of internal damping of austenitic steel in different states
A brief introduction to Judd-Ofelt theory: Application to rare earth-doped silicate glass
Photo- and radioluminescence of willemite in ZnO-Al ₂ O ₃ -SiO ₂ glass system
Influence of cutting tool geometry on machined surface roughness when machining thin-walled components from Inconel 718 manufactured by WAAM
All-inorganic perovskite quantum dots: a fundamental building block for optical neuromorphic synapse devices
Influence of Ga/Al Ratio on Luminescence and Scintillation in Ce3+/Tb3+ Co-Doped Gd3(Ga,Al)5O12 Scintillators
Effect of long-term exposure to chloride-containing solution on degradation of plasma-nitrided layer on AISI 316L stainless steel
<u>Viera Zatkalíková</u> , Lenka Markovičová, Martin Slezák, Milan Uhríčik, and Martin Vicen
Design and Development of a Transfer Cassette for Air-Sensitive Hazardous Materials in High Vacuum Ion Beam Systems
Compositional analysis of NaCl by thermoanalytical, structural, and optical methods for controlled combustion of nanodiamond particles
Author index71
List of Participants

PROGRAM

Monday, 8 September 2025

12:30	_	14:45	Registration
			Location: Hotel Lounge (near reception)
15:00	-	15:05	Opening Location: Lecture Hall
15:05	_	16:00	Monday Session I Location: Lecture Hall (chairperson: Zdeněk Kožíšek)
15:05	_	15:40	Vítězslav Jarý Where No One Else Dares: Growing Bulk Sulfide Single Crystals
15:40	-	16:00	Mária Behúlová Influence of argon shielding gas flow rate on the cooling and solidification of AA5087 aluminum alloy during wire arc additive manufacturing
16:00	-	16:30	Coffee break
16:30	_	18:10	Monday Session 2
			Location: Lecture Hall
			(chairperson: Mária Behúlová)
16:30	_	16:50	(chairperson: Mária Behúlová) Ladislav Koudelka Structure and properties of silver phosphate glasses with tungsten trioxide
16:30 16:50	_	16:50 17:10	Ladislav Koudelka
16:50	_		Ladislav Koudelka Structure and properties of silver phosphate glasses with tungsten trioxide Tomáš Hostinský
16:50	-	17:10	Ladislav Koudelka Structure and properties of silver phosphate glasses with tungsten trioxide Tomáš Hostinský Pushing limits of Mixed Glass Former Effect in Lithium Borophosphate glasses Shelja Sharma Structural, Morphological, and Optical Analysis of High-Purity ZnO Micro-
16:50 17:10	-	17:10 17:30	Ladislav Koudelka Structure and properties of silver phosphate glasses with tungsten trioxide Tomáš Hostinský Pushing limits of Mixed Glass Former Effect in Lithium Borophosphate glasses Shelja Sharma Structural, Morphological, and Optical Analysis of High-Purity ZnO Microrods Jakub Pilař

Tuesday, 9 September 2025

08:45	_	10:00	Tuesday Session 1
			Location: Lecture Hall
			(chairperson: Herbert Kindl)
08:45	_	09:20	Kei Kamada Development of crucible free crystal growth technique for high melting tem- perature oxide materials
09:20	-	09:40	Masao Yoshino Influence of Ga/Al Ratio on Luminescence and Scintillation in Ce3+/Tb3+ Co- Doped Gd3(Ga,Al)5O12 Scintillators
09:40	_	10:00	Hisato Suezumi Single Crystal Growth of Mg and Ce co-doped $Y_3(Ga,Al)_5O_{12}$ with various Mg concentration and their scintillation properties
10:00	_	10:30	Coffee break
10:30	_	11:50	Tuesday Session 2
			Location: Lecture Hall
			(chairperson: Kei Kamada)
10:30	_	10:50	Ryosuke Kawabata Monovalent ion doping effect on the scintillation properties of BaCl ₂ single crystals for eutectic type thermal neutron detector
10:50	_	11:10	Yuhei Nakata Study of the effect of plate thickness on spatial resolution in novel optical guid- ing crystal scintillator
11:10	_	11:30	Naveenkarthik Murugesan Ionic Conductivity of $Ln1$ - x Ae x F3- x (Ln = Tb , Dy , Ho , and Ae = Ca , Sr) Tysonite-type Fluoride for Ion Conductive Solid-state Electrolyte
11:30	_	11:50	Herbert Kindl Development and characterization of nanoparticle-infused glass rods prepared via the micro-pulling-down method
12:15	-	13:15	Lunch
14:00	_	15:40	Tuesday Session 3 Location: Lecture Hall (chairperson: Tomáš Hostinský)
14:00	-	14:20	Zdeněk Kožíšek A review of nucleation models in various systems
14:20	-	14:40	Tereza Machajdíková Application of finite difference method in solving phase-field models

14:40	_	15:00	Jakub Ježek Construction of Wannier orbitals and calculation of crystal field parameters of Ce-doped $Y_3Al_5O_{12}$
15:00	-	15:20	Petr Vařák A brief introduction to Judd-Ofelt theory: Application to rare earth-doped silicate glass
15:20	_	15:40	Milena Kubišová Statistical evaluation of metal plated polymer surfaces
15:40	-	16:10	Coffee break
16:10	_	18:10	Tuesday Session 4
			Location: Lecture Hall
			(chairperson: Tereza Machajdíková)
16:10	_	16:30	Vladimír Jorík Nonstandard use of powder diffraction methods for qualitative phase analysis
16:30	_	16:50	Rastislav Ďuriš The determination of the material properties using DIC
16:50	-	17:10	Kateřina Křehlíková Red-emitting Li ₂ MnCl ₄ for neutron detection: crystal growth and new doping strategies
17:10	-	17:30	Petra Zemenová Compositional analysis of NaCl by thermoanalytical, structural, and optical
			methods for controlled combustion of nanodiamond particles
17:30	-	17:50	Margita Ščasná Isotherm Study of Metribuzin and Tebuconazole Adsorption on Various Car-
			bonaceous Materials
17:50	_	18:10	Margita Ščasná Comparative Study of Selected Decontamination Agents for Surface Decontamination of Radionuclides
18:15	_	19:15	Dinner

Wednesday, 10 September 2025

08:45 - 10:00 Wednesday Session 1 Location: Lecture Hall (chairperson: Zdeněk Remeš) 08:45 - 09:20 Yung-Chi Yao All-inorganic perovskite quantum dots: a fundamental building block for cal neuromorphic synapse devices 09:20 - 09:40 Yen-Fa Liao Development and Application of HAXPES at TPS 09:40 - 10:00 Libor Ďuriška Investigation of chemically induced degradation on the microstructur morphology of Li-ion battery cathode 10:00 - 10:30 Coffee break 10:30 - 12:10 Wednesday Session 2 Location: Lecture Hall (chairperson: Vladimír Jorík) 10:30 - 10:50 Eva Babalová Influence of Dual-Beam Laser Welding Parameters on the Geometry of plex Stainless Steel Butt Welds: A Numerical Approach 10:50 - 11:10 Ivona Černičková Comparison of structural changes in SAC305 and SAC108 lead-free se alloyed with gallium	
Location: Lecture Hall (chairperson: Zdeněk Remeš) 08:45 - 09:20 Yung-Chi Yao All-inorganic perovskite quantum dots: a fundamental building block for cal neuromorphic synapse devices 09:20 - 09:40 Yen-Fa Liao Development and Application of HAXPES at TPS 09:40 - 10:00 Libor Ďuriška Investigation of chemically induced degradation on the microstructur morphology of Li-ion battery cathode 10:00 - 10:30 Coffee break 10:30 - 12:10 Wednesday Session 2 Location: Lecture Hall (chairperson: Vladimír Jorík) 10:30 - 10:50 Eva Babalová Influence of Dual-Beam Laser Welding Parameters on the Geometry of plex Stainless Steel Butt Welds: A Numerical Approach 10:50 - 11:10 Ivona Černičková Comparison of structural changes in SAC305 and SAC108 lead-free so alloyed with gallium	
08:45 - 09:20 Yung-Chi Yao All-inorganic perovskite quantum dots: a fundamental building block for cal neuromorphic synapse devices 09:20 - 09:40 Yen-Fa Liao Development and Application of HAXPES at TPS 09:40 - 10:00 Libor Ďuriška Investigation of chemically induced degradation on the microstructur morphology of Li-ion battery cathode 10:00 - 10:30 Coffee break 10:30 - 12:10 Wednesday Session 2 Location: Lecture Hall (chairperson: Vladimír Jorík) 10:30 - 10:50 Eva Babalová Influence of Dual-Beam Laser Welding Parameters on the Geometry of plex Stainless Steel Butt Welds: A Numerical Approach 10:50 - 11:10 Ivona Černičková Comparison of structural changes in SAC305 and SAC108 lead-free se alloyed with gallium	
All-inorganic perovskite quantum dots: a fundamental building block for cal neuromorphic synapse devices 09:20 - 09:40 Yen-Fa Liao Development and Application of HAXPES at TPS 09:40 - 10:00 Libor Ďuriška Investigation of chemically induced degradation on the microstructur morphology of Li-ion battery cathode 10:00 - 10:30 Coffee break 10:30 - 12:10 Wednesday Session 2 Location: Lecture Hall (chairperson: Vladimír Jorík) 10:30 - 10:50 Eva Babalová Influence of Dual-Beam Laser Welding Parameters on the Geometry of plex Stainless Steel Butt Welds: A Numerical Approach 10:50 - 11:10 Ivona Černičková Comparison of structural changes in SAC305 and SAC108 lead-free stalloyed with gallium	
Development and Application of HAXPES at TPS 10:40 - 10:00 Libor Ďuriška Investigation of chemically induced degradation on the microstructur morphology of Li-ion battery cathode 10:00 - 10:30 Coffee break 10:30 - 12:10 Wednesday Session 2 Location: Lecture Hall (chairperson: Vladimír Jorík) 10:30 - 10:50 Eva Babalová Influence of Dual-Beam Laser Welding Parameters on the Geometry of plex Stainless Steel Butt Welds: A Numerical Approach 10:50 - 11:10 Ivona Černičková Comparison of structural changes in SAC305 and SAC108 lead-free se alloyed with gallium	or opti-
Investigation of chemically induced degradation on the microstructure morphology of Li-ion battery cathode 10:00 - 10:30 Coffee break 10:30 - 12:10 Wednesday Session 2 Location: Lecture Hall (chairperson: Vladimír Jorík) 10:30 - 10:50 Eva Babalová Influence of Dual-Beam Laser Welding Parameters on the Geometry of plex Stainless Steel Butt Welds: A Numerical Approach 10:50 - 11:10 Ivona Černičková Comparison of structural changes in SAC305 and SAC108 lead-free se alloyed with gallium	
10:30 – 12:10 Wednesday Session 2 Location: Lecture Hall (chairperson: Vladimír Jorík) 10:30 – 10:50 Eva Babalová Influence of Dual-Beam Laser Welding Parameters on the Geometry of plex Stainless Steel Butt Welds: A Numerical Approach 10:50 – 11:10 Ivona Černičková Comparison of structural changes in SAC305 and SAC108 lead-free sa alloyed with gallium	ure and
Location: Lecture Hall (chairperson: Vladimír Jorík) 10:30 – 10:50 Eva Babalová Influence of Dual-Beam Laser Welding Parameters on the Geometry of plex Stainless Steel Butt Welds: A Numerical Approach 10:50 – 11:10 Ivona Černičková Comparison of structural changes in SAC305 and SAC108 lead-free se alloyed with gallium	
(chairperson: Vladimír Jorík) 10:30 – 10:50 Eva Babalová Influence of Dual-Beam Laser Welding Parameters on the Geometry of plex Stainless Steel Butt Welds: A Numerical Approach 10:50 – 11:10 Ivona Černičková Comparison of structural changes in SAC305 and SAC108 lead-free se alloyed with gallium	
 10:30 - 10:50 Eva Babalová Influence of Dual-Beam Laser Welding Parameters on the Geometry of plex Stainless Steel Butt Welds: A Numerical Approach 10:50 - 11:10 Ivona Černičková Comparison of structural changes in SAC305 and SAC108 lead-free so alloyed with gallium 	
Influence of Dual-Beam Laser Welding Parameters on the Geometry of plex Stainless Steel Butt Welds: A Numerical Approach 10:50 – 11:10 Ivona Černičková Comparison of structural changes in SAC305 and SAC108 lead-free se alloyed with gallium	
Comparison of structural changes in SAC305 and SAC108 lead-free so alloyed with gallium	of a Du-
	solders
11:10 – 11:30 Viera Zatkalíková Effect of long-term exposure to chloride-containing solution on degradat plasma-nitrided layer on AISI 316L stainless steel	ation of
11:30 – 11:50 Lenka Markovičová Evaluation of the Physico-Mechanical Properties of ABS Polymer for Au tive Applications	lutomo-
11:50 – 12:10 Patrícia Danišovičová Influence of Bi addition on microstructure and thermal properties of SA solders	SAC108
12:15 - 13:15 Lunch	
13:00 – 17:00 Wednesday: Company stand Location: Hotel IRIS: Coffee Room	
13:00 – 17:00 Miroslav Kamenský TESTOVACÍ TECHNIKA s.r.o company presentation	
14:00 – 17:00 Joint meeting - panel discussion	
17:50 – 18:00 Confere photo	
Location: Hotel IRIS - Terrace	
18:00 – 19:00 Dinner	

19:45 – 23:30 Conference banquet

Location: Wine Vault

Thursday, 11 September 2025

09:00	-	10:00	Thursday Session 1
			Location: Lecture Hall
			(chairperson: Vítězslav Jarý)
09:00	-	09:20	Bohuslav Rezek Plasmonic absorption in metal-ZnO nanocomplexes.
09:20	-	09:40	Zdeněk Remeš Optical spectroscopy and surface properties of doped nanocrystalline ZnO thin films on interdigital electrodes
09:40	_	10:00	Jakub Volf Photo- and radioluminescence of willemite in ZnO-Al $_2O_3$ -SiO $_2$ glass system
10:00	-	10:30	Coffee break
10:30	_	12:10	Thursday Session 2
			Location: Lecture Hall
			(chairperson: Maroš Martinkovič)
10:30	-	10:50	Juraj Kajan The melt growth of Al_2O_3 /YAG composite doped with cerium by Horizontal Directed crystalisation using Al_2O_3 seed
10:50	-	11:10	Filip Ferenčík Crystallographic Orientation-Dependent Growth of Nanoparticles via Mag- netron Sputtering on monocrystalline Rutile TiO ₂
11:10	-	11:30	Jana Knedlová Analysis of the Laser Beam Trajectory and its Impact on the Cut in Material PMMA
11:30	_	11:50	Dagmar Endlerová Optimization of the 3D freeforming process of PIM feedstock in granular form
11:50	-	12:10	Vladimír Šimna Analysis of Wire Electrode Wear in the WEDM Machining of Inconel 625
12:15	_	13:15	Lunch
14:00	_	16:00	Thursday Session 3
			Location: Lecture Hall
			(chairperson: Juraj Kajan)
14:00	-	14:20	Maroš Martinkovič Influence of welding parameters on the microstructure and properties of laser welds of duplex steels
14:20	-	14:40	Marek Vozár Influence of cutting tool geometry on machined surface roughness when ma- chining thin-walled components from Inconel 718 manufactured by WAAM

14:40	-	15:00	Milan Uhríčik Analysis of causes of cracking of piston rings mad of graphite cast iron
15:00	-	15:20	Milan Uhríčik Temperature dependence of internal damping of austenitic steel in different states
15:20	-	15:40	Matej Kubiš Design and optimization of a rotating sample holder for high-temperature ion implantation
15:40	-	16:00	Boris Pätoprstý Drag finishing as a post-treatment process of increasing the cobalt content in cemented carbide after plasma polishing
16:00	-	16:30	Coffee break
16:30	-	17:30	Thursday Session 4 (video session) Location: Lecture Hall (chairperson: Mária Behúlová)
16:30 16:30		17:30 16:50	Location: Lecture Hall
16:30	_		Location: Lecture Hall (chairperson: Mária Behúlová) Eva Labašová
16:30 16:50	-	16:50	Location: Lecture Hall (chairperson: Mária Behúlová) Eva Labašová Reliability of multi-state repairable systems Janette Kotianová

Friday, 12 September 2025

09:00	-	10:00	Friday Session 1
			Location: Lecture Hall
			(chairperson: Rastislav Ďuriš)
09:00	_	09:20	Adam Říha Measurement of Thermally Induced Depolarization in Flash-lamp Pumped Nd:YAG Laser Rod
09:20	-	09:40	Jan Kratochvíl Laser performance overview of rare-earth doped multicomponent garnet crystal $Gd_3(Ga,Al)_5O_{12}$
09:40	_	10:00	Dominika Popelová Micro-pulling-down grown Tm,Ho:GSAG crystal as laser gain medium
10:00	-	10:30	Coffee break
10:30	_	11:30	Friday Session 2
			Location: Lecture Hall
			(chairperson: Zdeněk Kožíšek)
10:30	_	10:50	Pavlína Zavadilová Design and Development of a Transfer Cassette for Air-Sensitive Hazardous
			Materials in High Vacuum Ion Beam Systems
10:50	_	11:10	František Jurina Influence of cutting edge microgeometry on the cutting forces and surface roughness of machining difficult-to-cut materials
11:10	-	11:30	Kateřina Rubešová Lutetium hafnates: From ceramics to OFZ-grown single crystals
11:50	_	12:00	Closing
			Location: Lecture Hall
12:00	-	13:00	Lunch

ABSTRACTS

Using Cayley graphs in costruction of large scale computer networks

Marcel Abas

Slovak University of Technology in Bratislava, Faculty of Materials Science and Technology in Trnava, Jána Bottu 2781/25, Trnava, 917 24, Slovakia

Nowadays, large-scale computing systems – such as supercomputers, cloud platforms, data centers, and parallel processing systems – can contain thousands or even millions of interconnected processors. Designing such networks requires careful attention to latency, efficiency, scalability, and fault tolerance, thus the communication network architecture is critical. One of the central challenges in this domain is minimizing communication delays while limiting the number of direct connections per node, since each connection incurs both physical and management costs.

The degree-diameter problem is defined as follows: given diameter d and maximum degree k, determine a graph with largest possible number of vertices satisfying these constraints. Graph theory provides a rigorous framework for modeling networks, where vertices correspond to computing devices and edges represent communication links. The degree-diameter problem is therefore particularly relevant in this context, as it captures the trade-off between node degree and communication efficiency.

For given finite group Γ and a unit-free inverse-closed generating set X, the vertex set of the Cayley graph $Cay(\Gamma,X)$ is Γ and there is an edge between g and gx for each $g\in\Gamma$ and $x\in X$. This paper examines the application of Cayley graphs to the construction of efficient large-scale computer networks. Cayley graphs, derived from group-theoretic principles, are vertex-transitive and regular, and they lend themselves to algebraic analysis. These properties make them attractive for designing network topologies with predictable, uniform behavior and efficient routing. We survey known results on small-diameter Cayley graphs and illustrate how they can be used to model interconnection networks that offer advantages such as symmetry, fault tolerance, and simplicity of routing algorithms.

We present several examples of modeling computing systems using Cayley graphs, focusing on key structural properties that make them suitable for large-scale networks. In particular, we highlight the use of diameter-two Cayley graphs (for example as described in [1] in the construction of networks that are both scalable and efficient.

[1] M. Abas, *Cayley graphs of diameter two with order greater than 0.684 of the Moore bound for any degree*, European Journal of Combinatorics, **57**, (2016), 109–120

Influence of Dual-Beam Laser Welding Parameters on the Geometry of a Duplex Stainless Steel Butt Welds: A Numerical Approach

Eva Babalová, Mária Behúlová, and Beáta Šimeková

Slovak University of Technology in Bratislava, Faculty of Materials Science and Technology in Trnava, ul. Jána Bottu Č. 2781/25, 91724 Trnava, Slovakia

Laser beam welding (LBW) has become a widely adopted method for joining duplex stainless steels (DSS) due to its high energy density, precise heat input control, and ability to produce welds with minimal thermal distortion and narrow heat-affected zones (HAZ). In recent developments, dual laser beam welding (DLBW), particularly in twin-spot configurations, has gained increased attention for its enhanced control over the thermal profile during welding. By varying the power ratio and spatial offset between the two laser beams, it is possible to manipulate temperature gradients and tailor solidification dynamics. This level of control is essential for maintaining the optimal austenite-to-ferrite phase balance in the weld metal, thereby ensuring the mechanical integrity and corrosion resistance of the welded joint [1-3].

This study examines the effect of process parameters on weld size and geometry during DLBW of DSS 2304 (EN 1.4362) using finite element modeling (FEM). Simulations were performed in ANSYS 2022 R2 with beam power ratios of 50:50, 20:80, and 80:20. A 3D model of 5 mm thick welded sheets was created, incorporating refined meshing along the weld path. Thermophysical properties were obtained from JMatPro v6.1.

A conical volumetric heat source represented the twin beams in a tandem setup, with third-kind boundary conditions applied to simulate convective and radiative cooling. Temperature field predictions were validated against weld macrostructures. Mechanical properties were assessed through tensile testing and microhardness measurements.

The results demonstrate that DLBW process parameters significantly influence weld geometry and thermal behavior. The FEM approach proved effective for optimizing welding conditions to achieve defect-free joints with desirable mechanical properties.

- [1] L. Pezzato, I. Calliari. Advances in duplex stainless steels. Materials 15, 20 (2022) 7132.
- [2] A. Higelin, S. Le Manchet, G. Passot et al. Heat-affected zone ferrite content control of a duplex stainless steel grade to enhance weldability. Weld World 66 (2022) 1503–1519.
- [3] D. A. Efa. Enhancing the efficiency of laser beam welding, multi-objective parametric optimization of dissimilar materials using finite element analysis. Int. J. Adv. Manuf. Technol. 133 (2024) 4525-4541.

Influence of argon shielding gas flow rate on the cooling and solidification of AA5087 aluminum alloy during wire arc additive manufacturing

<u>Mária Behúlová</u>¹, Eva Babalová¹, Marián Pavlík¹, and Miroslav Sahul²

¹Slovak University of Technology in Bratislava, Faculty of Materials Science and Technology in Trnava, Ulica Jána Bottu č. 2781/25, 917 24 Trnava, Slovakia

²Czech Technical University in Prague, Faculty of Mechanical Engineering, Technická 4, 166 07

Praha 6, Czech Republic

Wire Arc Additive Manufacturing based on Metal Inert Gas welding (WAAM-MIG) has emerged as a cost-effective technique for fabricating large-scale aluminum alloy components [1-4]. However, the deposition process is strongly influenced by process parameters that govern thermal behavior and layer formation. Among these parameters, the argon shielding gas flow rate plays a critical role - not only in controlling cooling and solidification rates, but also in stabilizing the arc, thereby influencing the geometry of individual layers [5-6].

This study investigates the combined effects of argon flow on thermal gradients, bead morphology, and dimensional stability during WAAM-MIG production of an AA5087 aluminum alloy component, using both numerical simulation in ANSYS software and experimental validation. The deposition process of ESAB OK Autrod 5087 filler wire, with a diameter of 1.2 mm, onto the surface of an AW5083 aluminum plate with a thickness of 4 mm was carried out using a Fronius TPS600i welding power source, with a welding current of 65 A and a voltage of 16.1 V. Argon shielding gas at flow rates ranging from 6 L.min⁻¹ to 14 L.min⁻¹ was applied, along with a constant travel speed of 5 mm.s⁻¹ and a wire feed speed of 4 m.min⁻¹. The produced weld bead had a length of 100 mm.

At lower argon flow rates, insufficient shielding leads to broader, flatter layers due to extended melt pool spreading. In contrast, excessive flow can disturb the molten pool, resulting in irregular and elevated beads. The obtained results show that an optimal gas flow rate enhances convective heat extraction, promoting refined microstructures and consistent bead geometry. The findings demonstrate that argon gas flow rate directly affects bead height, width, and surface uniformity, with significant implications for geometric accuracy and mechanical properties of the final components. This work underscores the importance of optimizing shielding gas dynamics to achieve both desirable microstructural characteristics and dimensional precision in WAAM-fabricated AA5087 parts.

- [1] A. Shah, R. Aliyev, H. Zeidler, S. Krinke, J. Manuf. Mater. Process. 7, 97 (2023).
- [2] B. Tomar, S. Shiva and T. Nath, Mater. Today Commun. 31, 103739 (2022).
- [3] X. Zhu et al., Mater. Today Commun. 43, 111778 (2025).
- [4] C. R. Cunningham et al., Addit. Manuf. 22, 672 (2018).
- [5] M. Arana et al., Metals 11, 524 (2021).
- [6] T. Hauser et al,. Addit. Manuf. 41, 101993 (2021).

Comparison of structural changes in SAC305 and SAC108 lead-free solders alloyed with gallium

<u>Ivona Černičková</u>, Libor Ďuriška, Patrícia Danišovičová, Marián Drienovský, Terézia Machajdíková, Michaela Halmanová, and Roman Čička

Slovak University of Technology in Bratislava, Faculty of Materials Science and Technology in Trnava, Ulica Jána Bottu č. 2781/25, 917 24 Trnava, Slovakia

The aim of the work is to study structural changes in SAC305 and SAC108 lead-free solders alloyed with gallium and to compare the experimental results. In the experimental investigation, scanning electron microscopy, energy-dispersive X-ray spectroscopy, X-ray diffraction and differential scanning calorimetry were used. Influence of addition of gallium in the SAC305 and SAC108 solders on their microstructure and thermal properties will be observed. The main emphasis will be placed on the evaluation of structural changes in Ag-rich and Cu-rich intermetallic phases with respect to the Ga content.

Influence of Bi addition on microstructure and thermal properties of SAC108 solders

<u>Patrícia Danišovičová</u>, Marián Drienovský, Libor Ďuriška, Michaela Halmanová, and Ivona Černičková

Slovak University of Technology in Bratislava Faculty of Materials Science and T, Ulica Jána Bottu Trnava, Trnava, Slovakia

Solders are essential for creating strong, conductive joints in electronic circuits without damaging sensitive components. Sn-Pb eutectic solder alloy has been widely used in the electronics industry due to its suitable mechanical and thermal properties [1]. However, global restrictions on lead-containing solders, driven by environmental and health regulations, have necessitated the development of alternative soldering alloys [2]. Various lead-free solder alloys have been proposed, including Sn-Ag, Sn-Ag-Cu, Sn-Cu, Sn-Zn, and Sn-Bi systems. Among these, Sn-Bi based solder alloys have attracted considerable attention due to their lower melting temperatures, good tensile strength, and excellent creep resistance, making them promising candidates to replace traditional lead-based solders [3]. The aim of this work was to study the influence of Bi addition on the microstructure and thermal properties of SAC108 lead-free solders. In this investigation, scanning electron microscopy, energy-dispersive spectroscopy, and differential scanning calorimetry were used. The addition of Bi resulted in a lowering of the melting temperature. Microstructural changes were also observed, such as the formation of Bi globular particles at the boundaries between the matrix and minor intermetallic phases.

- [1] Abtew, M. and Selvaduray, G. Lead-free solders in microelectronics, Mater Sci Eng R Rep, 27 (2000): pp 95-141
- [2] Y. Yao, X. Long, L. M. Keer, A Rev. of Rec. Research on the Mech. Behavior od Lead-Free Solders (2017)
- [3] Chen X. Feng, X, Zhou J, Yao Y. Effect of In on microstructure, thermodynamic characteristic and mechanical properties of Sn–Bi based lead-free solder (2015); Journal of Alloys and Compounds. Volume 633

The determination of the material properties using DIC

Rastislav Ďuriš

Slovak University of Technology in Bratislava, Faculty of Materials Science and Technology in Trnava, Ulica Jána Bottu č. 2781/25, 917 24 Trnava, Slovakia

Nowadays, the strain gauge method or other contact methods of measuring deformation are often replaced by optical deformation measurement techniques. Among the most common and universally applicable optical non-contact methods is currently digital image correlation (DIC). The developed computational correlation algorithms allow to track the movement of material points in set of images capturing the deformation process with sufficient accuracy. This allow to obtain a sufficiently reliable estimate of the distribution of deformation fields. Therefore, the optical method of digital image correlation can be used to measure deformations in various applications, such as: monitoring the condition of structures, monitoring the growth of fatigue cracks, testing at high temperatures, etc. where the use of standard methods is difficult or financially expensive. The adaptability of the DIC technique lies in the possibility capture of images with standard cameras, applicability to a wide range of dimensions and materials of tested samples and structures.

The paper focuses on the use of open source MATLAB 2D DIC software Ncorr to evaluate the deformations of a test sample during a static tensile test. The results of the uniaxial strain estimation obtained by the DIC method were verified by experimental measurements using an installed strain gauge and a reference extensometer. Subsequently, the Ncorr software was extended with functions enabling the determination of the basic material parameters of the samples: Young's modulus of elasticity and Poisson's ratio.

Investigation of chemically induced degradation on the microstructure and morphology of Li-ion battery cathode

<u>Libor Ďuriška</u>¹, Ivona Černičková¹, Jakub Rafajdus¹, Martin Kusý¹, Marián Drienovský¹, Lenka Blinová¹, Santanu Mukherjee², and Jakub Reiter²

¹Slovak University of Technology in Bratislava, Faculty of Materials Science and Technology in Trnava, Ulica Jána Bottu č. 2781/25, 917 24 Trnava, Slovakia

²InoBat Auto j.s.a., Voderady 429, 919 42 Voderady, Slovakia

Nowadays, $\text{LiNi}_x\text{Co}_y\text{Mn}_{1-x-y}\text{O}_2$ (NMC) is one of the most widely used active cathode materials (CAM) for Li-ion batteries in automotive, mainly due to its high specific capacity combined with low manufacturing costs. However, NMC cathode materials are sensitive to air due to their tendency to absorb moisture and react with CO $\,$, forming surface layers that degrade battery performance. Highnickel compositions are especially unstable, leading to surface reactions and structural degradation in ambient conditions [1-3].

The aim of this work was to investigate the NMC811 cathode in pristine condition as well as after its storage under exposure of ambient atmosphere at room temperature and humidity for progressively increasing times (1, 2 and 3 months). Microstructure and morphology of the cathode in both top view and cross-section were observed using scanning electron microscopy (SEM), the distribution of elements was mapped by means of energy-dispersive X-ray spectroscopy (EDX). The structure of cathode active material was identified by X-ray diffraction (XRD), using two configurations: Theta-2Theta, Grazing incidence. The phase transformations during heating and cooling were analyzed by differential scanning calorimetry (DSC), while mass changes by thermogravimetry (TGA). To evaluate the functional groups on the surface of the cathode, the Fourier-transformed infrared spectroscopy (FTIR) was used.

The results showed that impurities appeared in the cathode after exposure to ambient conditions and their amount increased with longer exposure time. Structural changes were also observed, which were more pronounced at the surface compared to the bulk.

- [1] B. Xu et al., Mater. Sci. Eng.: R: Rep. 73 (2012) 51–65.
- [2] W. Li et al., Chem. Soc. Rev. 46 (2017) 3006–3059.
- [3] W. Li et al., Nat. Energy 5 (2020) 26–34.

Optimization of the 3D freeforming process of PIM feedstock in granular form

Dagmar Endlerová¹, Berenika Hausnerová¹, Martin Novák², Vojtěch Šenkeřík¹, and Vladimír Pata¹

¹Tomas Bata University in Zlín, Faculty of technology, Vavrečkova 5669, 760 01 Zlín, Czechia ²Tomas Bata University in Zlín, Centre of Polymer Systems, třída Tomáše Bati 5678, 760 01 Zlín, Czechia

This work describes the development of a hybrid material optimized for processing by two different technologies: powder injection molding (PIM) and 3D extrusion. The aim is to design and optimize the 3D extrusion parameters of a PIM-grade feedstock in order to produce printed parts with acceptable surface roughness prior to sintering. The feedstock consisted of iron carbonyl metal powder combined with an environmentally friendly wax-based binder. The critical solid loading was determined by torque analysis during compounding in a twin-screw mixer. To ensure the material's suitability for both injection molding and 3D printing, its flow behavior was analyzed using a capillary rheometer, which enabled the identification of appropriate processing parameters for both manufacturing methods.

Based on these parameters, test sets of samples were prepared by 3D extrusion as well as by conventional injection molding. The surface quality and morphology of the parts before sintering were evaluated using microscopic analysis, allowing a detailed comparison of both production methods. The results were further analyzed using advanced statistical tools to quantify differences in surface characteristics and to define the technological limitations and potential of the hybrid approach. This work contributes to a deeper understanding of the relationships between feedstock composition, flow behavior, and the resulting quality of pre-sintered parts produced by both additive and conventional technologies.

Keywords: powder injection molding, 3D freeforming, feedstock, hybrid material, surface roughness.

Crystallographic Orientation-Dependent Growth of Nanoparticles via Magnetron Sputtering on monocrystalline Rutile ${\rm TiO_2}$

Filip Ferenčík¹, Viliam Vretenár², Diana Fabušová¹, and Pavol Noga¹

¹Slovak University of Technology in Bratislava, Faculty of Materials Science and Technology in Trnava, ATRI, Ulica Jána Bottu č. 2781/25, 917 24 Trnava, Slovakia

²Centre for Nanodiagnostics of Materials, Faculty of Materials Science and Technology, Slovak University of Technology in Bratislava, Vazovova 5, Bratislava, 81243, Slovakia

This work presents a novel approach to the preparation of nanoparticles using magnetron sputtering on monocrystalline rutile ${\rm TiO_2}$ substrates with defined crystallographic orientation. We found that the crystallographic orientation of the substrate significantly influences the nucleation and growth processes of nanoparticles, resulting in particle sizes and ranging from a few to several tens of nanometers. The mechanisms of there processes and their effects on the characteristics of the nanoparticles are investigated using scanning and transmission electron microscopy combined with Auger Electron Spectroscopy and Time of Flight Elastic Recoil Detection Analysis. Our results provide new insights into the controlled synthesis of nanomaterials and open avenues for optimizing nanoparticle properties for specific applications. In particular, we focused on the formation of PdCu nanoparticles, which are wdely used in catalysis, especially in C-C coupling reactions. Our method offers a new route for their preparation and enables the study of the substrate-induced effects on nanoparticle characteristics.

Pushing limits of Mixed Glass Former Effect in Lithium Borophosphate glasses

Tomáš Hostinský, Ladislav Koudelka, and Petr Mošner

University of Pardubice, Faculty of Chemical Technology, Department of General and Inorganic Chemistry, Studentská 573, 532 10 Pardubice, Czechia

The mixed glass former effect (MGFE) offers a promising strategy for tailoring the structure and functional properties of amorphous solids. In this study, we explore its limits through systematic compositional tuning of lithium borophosphate glasses within the $40\text{Li}_2\text{O}$ -zWO₃-[(60-z)/4*(3P₂O₅-1B₂O₃)] system. By progressively substituting borate and phosphate units with tungsten oxide while maintaining a fixed P₂O₅:B₂O₃ ratio, we investigate how such dual substitution influences structural evolution and ionic conductivity.

Comprehensive characterization using density and thermal analysis, Raman spectroscopy, and advanced 1D and 2D MAS NMR techniques reveals a gradual transformation from a phosphate-borate to a tungstate-dominated glass network. This shift is accompanied by significant structural depolymerisation, including the formation of isolated phosphate and borate units, emergence of W-O-W linkages, and the growth of mixed tungstate species such as Q^0 , Q^1 , and B-O-W environments.

Impedance spectroscopy measurements show a remarkable three-order-of-magnitude increase in room-temperature DC conductivity (from 10^{-9} to $10^{-6}~\Omega^{-1}*cm^{-1}$) across the compositional series. This enhancement is directly linked to the evolving glass structure, which facilitates lithium ion mobility through the disruption of rigid phosphate and borophosphate networks and the formation of more accessible conduction pathways.

Our findings confirm that strategic control over glass former composition enables continuous and predictable optimization of ionic transport. These results not only extend the conceptual framework of the MGFE but also demonstrate a viable path for developing high-performance solid electrolytes based on borophosphate glasses.

Analysis of causes of cracking of piston rings mad of graphite cast iron

Silvia Hudecová, <u>Milan Uhríčik</u>, Peter Palček, Veronika Chvalníková, Martin Slezák, Zuzana Šurdová, Edita Illichmanová, and Lukáš Šikyňa

University of Žilina, Faculty of Mechanical Engineering, Department of Materials Engineering, Univerzitná 8125/1, 010 26 Žilina, Slovakia

Piston rings are key components of internal combustion engines, which provide a seal between the piston and the cylinder, thereby significantly affecting the performance, reliability and service life of the engine. Rings made of graphite cast iron are often used in practice, mainly due to their favorable tribological properties, wear resistance and good self-lubricating capabilities. Despite these advantages, cases of premature failure of these components in the form of cracks and subsequent fracture may occur in operation [1, 2].

The aim is to identify and analyze the main causes of cracking of piston rings made of graphite cast iron, by combining experimental and analytical approaches. The work presents macroscopic and microscopic analysis of fracture surfaces, metallographic and fractographic observation, as well as results from chemical analysis of the material. Special attention is paid to the nature of the graphite shape.

The findings contribute to a deeper understanding of degradation mechanisms in piston rings and offer recommendations for optimizing the manufacturing process, choosing the appropriate microstructure and operating conditions in order to increase their service life and reliability.

- [1] A. Diószegi, V. Fourlakidis, and I.L. Svensson, Mater. Scien. For. 649 (2010) 517.
- [2] H. Yamagata, The Scie. And Tech. of Mat. In Aut. Eng. (2005) 87.

Where No One Else Dares: Growing Bulk Sulfide Single Crystals

Vítězslav Jarý¹, Lubomír Havlák¹, Jan Bárta^{1,2}, Vojtěch Vaněček¹, Robert Král¹, and Jakub Ježek¹

As it was stated in famous Smet's review paper "Luminescence in Sulfides: A Rich History and a Bright Future", sulfide-based luminescent materials have attracted a lot of attention for a wide range of photo, cathodo- and electroluminescent applications [1]. They feature narrow band gaps and low phonon energy, and compared to their oxide counterparts, they exhibit greater covalency and atomic overlap due to the diffuse nature of sulfur's orbitals, which is, in part, attributed to its lower electronegativity. This leads to complementary properties, such as increased hole mobility and narrower electronic band gaps [1,2]. Another significant aspect of sulfides lies in their structural chemistry. The presence of larger sulfur ions, with a radius of 1.8 Å, stabilizes metal sulfides in lower symmetry structures with lower coordination numbers [3].

From the technological standpoint, sulfides have "the worst of both worlds" of halides and oxides. Similarly to halides, sulfides tend to react with oxygen and water at elevated temperatures to form very stable oxysulfides. Like oxides, sulfides often possess high melting points, but unlike oxides, they react with high melting metals used as crucible materials for oxide single crystal growth. This presents a significant limitation for growing high-quality sulfide crystals. However, our team possesses high-temperature annealing technology in a sulphonating atmosphere. The combination of the above-mentioned properties makes the growth of sulfide bulk crystals a challenging task.

In this presentation, a significant contribution to the sulfide crystal growth and research at the Institute of Physics of the Czech academy of sciences, will be acknowledged. Special attention will be given to crystalline platelets of ternary sulfide of general formula $ALnS_2$ (A = alkali metal, Ln = La, Gd, Lu, Y) [4] and single crystals of Pr^{3+} -doped Lu_2S_3 [5], as we are the only laboratory in the world carrying on systematic research of these highly interesting compounds. Special attention will be given to the ways of crystal preparation, followed by detailed characterization of their structural and luminescence properties, mainly by means of time-resolved luminescence spectroscopy. Applications mainly in the fields of fast-scintillators, white solid state LEDs or mid-infrared lasers will be addressed as well.

- [1] P. F. Smet et al. Materials 3(4), 2010, 2834-2883
- [2] B. J. Moore et al. CrystEngComm 26, 2024, 1444-1452
- [3] M. R. Harrison et al. Coordination Chemistry Reviews 255, 2011, 451-458
- [4] V. Jarý et al. Physical Review Applied 19, 2023, 034092
- [5] V. Vaněček et al. Crystal Growth and Design 24(11), 2024, 4736-4742

¹Institute of Physics of the Czech Academy of Sciences, Cukrovarnická 10/112, Prague 6, Czechia ²Faculty of Nuclear Sciences and Physical Engineering, Czech Technical University in Prague, Břehová 7, Praha 1, Prague 11519, Czechia

Construction of Wannier orbitals and calculation of crystal field parameters of Ce-doped $Y_3Al_5O_{12}$

<u>Jakub Ježek</u>^{1,2} and David Sedmidubský²

¹Institute of Physics of the Czech Academy of Sciences, Na Slovance 1999/2, 182 00 Prague 8, Czechia

When studying the electronic structure of inorganic crystals using Density Functional Theory (DFT) in Periodic Boundary Conditions (PBC), Bloch orbitals $\psi_{n,\mathbf{k}}(\mathbf{r})$ are typically employed to better describe electron delocalization in solids compared to Gaussian orbitals. Bloch orbitals are characterized by two quantum numbers: n (band index) and \mathbf{k} (wave vector within the first Brillouin zone). However, for materials containing lanthanides, the 4f and 5d bands tend to be highly localized, making it challenging to accurately estimate intra-band energies of the ground state. This limitation can be addressed by using Wannier orbitals $\mathbf{w}_n(\mathbf{r}-\mathbf{R})$, which are localized on atoms at position vector \mathbf{R} . Transformation to Wannier orbitals enables the extraction of crystal field parameters (CFP) and facilitates calculations of crystal field splitting effects within the local atomic Hamiltonian ansatz.

In this work, the previously developed methodology of CFP extraction through Wannierization of APW-based Bloch functions (calculated by Wien2k code) is combined with the atomic Hamiltonian constructed using Stevens operator equivalents applied on M_J basis set of a given multiplet. This approach is demonstrated on the well known system of Ce-doped $Y_3Al_5O_{12}$ garnet (YAG:Ce) as a test case. Moreover, an atempt is made to assess the effective electron correlation parameter U for Ce-4f states using a similar technique as in CFP analysis, namely bringing the 4f states from valence shell to core. The 4f-4f electronic transitions estimated from crystal field splitting, spin-orbit interaction and possibly electron correlations will be compared with standard DFT+U band structure calculations to highlight the enhanced information content and chemical interpretability achievable through this localization approach. While YAG:Ce is well-characterized experimentally, it might serve as an ideal benchmark system to validate the applicability of Wannier-based crystal field analysis combined with operator equivalent approach, potentially opening new computational pathways for studying less well-known lanthanide-doped materials with improved chemical insight.

- [1] P. Blaha, K. Schwarz, G. Madsen, D. Kvasnicka, and J. Luitz, WIEN2k: An Augmented Plane Wave plus Local Orbitals Program for Calculating Crystal Properties (Technische Universität Wien, Wien, 2001).
- [2] A. A. Mostofi, J. R. Yates, Y.-S. Lee, I. Souza, D. Vanderbilt, and N. Marzari, Comput. Phys. Commun. 178 (2008) 685
- [3] E. Mihóková, P. Novák, and V. V. Laguta, J. Rare Earths 33 (2015) 1316

²Department of Inorganic Chemistry, University of Chemistry and Technology, Technická 5, 166 28 Prague 6, Czechia

Nonstandard use of powder diffraction methods for qualitative phase analysis

Vladimír Jorík and Miroslava Puchoňová

Slovak University of Technology, Radlinského 9, Bratislava, Slovakia

Interpretation of the powder diffractogram can be a simple or complex operation depending on the number and structural complexity of the phases that make up the sample and the amount and nature of the information required. A relatively simple way of interpreting the diffractogram is to compare it with the diffractogram of the reference material. To do this, it is generally required to calculate the interplanar distances belonging to the different diffraction lines, and less often it is necessary to determine the diffraction indices.

Qualitative phase analysis provides elementary chemical information about a substance just like many other analytical methods. However, what distinguishes powder diffraction methods from them is their unique ability to characterize crystalline phases. It is based on the following principles:

- Each crystalline substance is characterized by a unique diffraction pattern
- Each substance in the mixture produces its diffractogram independently of the others
- The identification of the crystalline phase is based on its chemical structure

Other advantages of powder diffraction analysis for "chemical analysis" are its non-destructive nature, only a small amount of the substance needed for analysis and the possibility to develop it for semi-quantitative analysis.

Standard qualitative phase analysis is performed by comparing the diffractogram of an unknown sample with a set of reference powder diffractograms. The same principle applies to crystalline mixtures, in which the diffractogram of the identified component is "subtracted" from the diffraction pattern of the mixture and the identification process continues with the remaining diffraction lines until all lines are completely assigned. The key role here is the existence (availability) of a sufficiently large, well-organized library (database) of reference powder diffractograms, continuously updated with high-quality diffraction data. The ICDD PDF powder database currently meets these criteria.

Among the non-standard procedures of qualitative phase analysis, we can include:

Crystallographic analysis focused on the processing of basic experimental data, from which it allows to obtain basic crystallographic information about the investigated substance. These include interplanar distances d_{hkl} of individual lattice planes, diffraction indices h, k, l, dimensions of the basic parallelepiped (lattice parameters a, b, c, α , β , γ), type of crystal lattice and diffraction intensities.

Le Bail analysis, which is a method of refining the crystal structure by comparing the whole digitized experimental powder pattern with the digitized calculated powder diffraction pattern.

A major benefit of non-standard qualitative phase analysis procedures is that, in addition to the possibility of identifying a known crystalline phase, they provide additional information on the investigated substance. These can often be used to correlate with some of the physical properties that can be used in technological and research practice.

Influence of cutting edge microgeometry on the cutting forces and surface roughness of machining difficult-to-cut materials

František Jurina, Tomáš Vopát, Marek Vozár, Boris Pätoprstý, and Dominik Zajko

Slovak University of Technology in Bratislava, Faculty of Materials Science and Technology in Trnava, Ulica Jána Bottu č. 2781/25, 917 24 Trnava, Slovakia

The paper presents research investigating the influence of cutting tool microgeometry on cutting forces and machined surface roughness when milling the difficult-to-cut nickel alloy Inconel 718. Cemented carbide tools with different cutting edge rounding sizes (5, 8, 15, 30, and 45 μ m) were tested under defined cutting conditions for both roughing and finishing operations. Cutting forces were measured in-process using a piezoelectric dynamometer, while machined surface roughness parameters (Ra, Rq, Rz) were evaluated after machining using a contact profilometer. Previous research into cutting edge microgeometry suggests that modifying the cutting edge of milling tools can substantially extend effective tool life, reduce cutting forces during the process, and ensure higher quality of the machined surface.

The results showed that the smallest cutting edge rounding (5 μ m) led to lower initial cutting forces but faster wear progression. The larger roundings (15, 30, and 45 μ m) reduced the wear rate but increased cutting forces and worsened surface roughness. An optimal balance between tool life, cutting forces, and surface quality was achieved with the 8 μ m rounding.

The melt growth of Al₂O₃/YAG composite doped with cerium by Horizontal Directed crystalisation using Al₂O₃ seed

<u>Juraj Kajan</u>^{1,2}, Tomáš Gregor^{1,2}, Anna Prnová³, Peter Švančárek³, Grigori Damazyan², Jakub Michalík¹, Mykhailo Chaika⁴, and Dušan Galusek³

¹Institute of Competitiveness and Innovations, University of Žilina, Univerzitná 8215, 010 26 Žilina, Slovakia

²AT Crystals s.r.o., Rosinská cesta 9, Zilina 010 08, Slovakia

³Joint Glass Centre of the IIC SAS, TnUAD and FChPT STU, Trenčín, Študentská 2, 911 50 Trenčín, Slovakia

⁴Institute of Low Temperature and Structure Research, Polish Academy of Sciences, Okólna 2, Wrocław 50 – 422, Poland

A composite material based on eutectic ceramics Ce:YAG/Al O grown from the melt(MGC) was successfully obtained by the HDC method with dimensions of $220\times65\times25$ mm. In this work, the effect of using a sapphire seed on the inheritance of the texture orientation of the ingot was investigated. A single-phase sapphire seed with the M [10-10] axis was used to orient the ingot texture along the growth direction. SEM and EBSD methods showed that the orientation of sapphire lamellas could be successfully induced with the preservation of orientation throughout the entire volume of the ingot. These results can contribute to improving the properties of eutectic ceramic materials obtained from the melt.

Development of crucible free crystal growth technique for high melting temperature oxide materials

Kei Kamada

Tohoku University, 2-1-1 Katahira Sendai, Sendai, Japan

The abstract has not been sent.

TESTOVACÍ TECHNIKA s.r.o. - company presentation

Miroslav Kamenský

TESTOVACÍ TECHNIKA s.r.o., Československé armády 923/15, 290 01 Poděbrady, Czechia

Web site: https://teste.sk/

Monovalent ion doping effect on the scintillation properties of BaCl₂ single crystals for eutectic type thermal neutron detector

Ryosuke Kawabata^{1,2}, Masao Yoshino^{2,4}, Kei Kamada^{2,3,4}, Kyoung Jin Kim^{2,3,4}, Naoko Kutsuzawa⁴, Rikito Murakami^{2,4}, Akihiro Yamaji^{2,3}, Satoshi Ishizawa^{2,4}, Takashi Hanada², Yuui Yokota^{2,3}, Shunsuke Kurosawa^{2,3,5}, Hiroki Sato^{2,3}, and Akira Yoshikawa^{2,3,4}

¹Tohoku University, Graduate School of Engineering, Japan
²Institute for Materials Research, Tohoku University, Japan
³New Industry Creation Hatchery Center, Tohoku University, Japan
⁴C&A Corporation, Japan
⁵Institute of Laser Engineering, Osaka University, Japan

[Introduction] Demand for thermal neutron detectors is rising, especially for lithium-ion battery inspection and nuclear power plant dosimetry. While ³He gas detectors were standard due to their stability, recent resource depletion has created a significant supply-demand imbalance. To address this, ⁶Li-containing solid scintillators, leveraging the ⁶Li(n, α) reaction, are being developed. Eutectic scintillators, combining a ⁶Li neutron capture phases with scintillator phases, are particularly promising as ³He alternatives due to their high and flexible ⁶Li content. BaCl₂ is considered a promising candidate for a scintillator phase owing to its low hygroscopicity and a refractive index comparable to that of LiCl, which serves as the neutron capture phase. Previous studies have reported the use of Eu:LiCl/BaCl₂^[1], and Tb:BaCl₂/NaCl/KCl^[2] for X-ray detection. In reference [2], it was suggested that the luminescence properties of the BaCl₂ phase may have been enhanced by the trace incorporation of NaCl or KCl, which were blended with BaCl₂ to form a eutectic composite.^[3] The deliberate doping of trace amounts of monovalent cations such as Na⁺ or K⁺ into BaCl₂ and the subsequent analysis of its scintillation behavior are pivotal for optimizing the performance of the scintillator phase in eutectic-type thermal neutron detectors. Accordingly, the present study aimed to grow BaCl₂ crystals doped with Na, K, Tb, and Eu, characterize their scintillation properties, and assess their potential for practical implementation as a scintillator phase.

[Results] In the initial stage of this study, the effects of co-doping with monovalent cations on $BaCl_2$, which constitutes the scintillator phase, were systematically investigated. $BaCl_2$:K1% single crystal was grown by the VB method. The results of X-ray radioluminescence measurements demonstrated that the incorporation of monovalent potassium suppressed the self-trapped exciton (STE) emission near 300 nm, while enhancing the emission around 410 nm, which is associated with defects and impurities in $BaCl_2$. The scintillation pulse height spectra were measured under 137 Cs gamma-ray irradiation, revealing that $BaCl_2$:K1% exhibited a light output three times greater than that of undoped $BaCl_2$. The results of detailed crystal growth procedures and other scintillation properties will be presented in the conference.

- [1] Yui Takizawa et al 2022 Jpn. J. Appl. Phys. 61 SC1038
- [2] Yui Takizawa et al 2022 Jpn. J. Appl. Phys. 61 SC1009
- [3] Yui Takizawa et al., Journal of Crystal Growth 580 (2022) 126467
- [4] K. Onodera et al., Radiation Physics and Chemistry 78 (2009) 1031–1033

Development and characterization of nanoparticle-infused glass rods prepared via the micro-pulling-down method

Herbert Kindl^{1,2}, Karol Bartosiewicz¹, and František Zajíc¹

¹Institute of Physics of the Czech Academy of Sciences, Cukrovarnická 10/112, Prague, 162 00, Czechia

²Department of Inorganic Chemistry, University of Chemistry and Technology, Prague (UCT Prague), Technická 5, Prague 166 28, Czech Republic

This work focuses on the development of glass rods infused with various nanoparticles as a promising new radioluminescent material with fast timing. The motivation for preparing such material was to mitigate quenching effects caused by volume phenomena typically observed in bulk luminescent materials. This can be achieved by embedding crystalline nanoparticles of a luminescent material into a low-melting-point matrix. This strategy effectively reduces the impact of total internal reflection, which traps emitted photons within the crystal lattice and restricts their extraction. As light emission occurs independently from each nanoparticle within the system, this approach can enhance luminescence speed and efficiency. A method chosen for the preparation of these nanocomposites was the micro-pulling-down method (μ -PD). During the μ -PD process, the melt is pulled through a capillary in which microscopic cavities occur due to high pulling rates. As these cavities collapse, they release shock waves, effectively separating agglomerated nanoparticles. The main goal of this work was to optimize the growth process by customizing the hot zone and to determine the effects of different temperature and pulling rate programs on rod shape and nanoparticle distribution. Furthermore, samples will be characterized using XRD, SEM/EDS and optical, luminescent and scintillation properties will be estimated.

Analysis of the Laser Beam Trajectory and its Impact on the Cut in Material PMMA

Jana Knedlová, Ondřej Bílek, Michal Hanus, and David Bartík

Tomas Bata University in Zlín, Faculty of Technology, Vavrečkova 5669, 760 01 Zlín, Czechia

This article investigates the influence of laser beam trajectory on the final dimension of machined parts using the ILS 3NM $\rm CO_2$ laser system, operating at a wavelength of 10.6 μm with a maximum power output of 100 W and a maximum feed rate of 1524 mm \cdot s⁻¹. The study is conducted on 3 mm and 5 mm thick PMMA sheets using focusing lenses with focal lengths of 1.5 and 2.5 inches. Machining precision is evaluated by comparison circular and linear beam paths. The primary objective is to asses the impact of motion interpolation on machining quality and to determine how different focal lengths and material thicknesses influence the final dimensions of the workpiece.

Analysis of welding simulation results using DOE methodology

Janette Kotianová, Mária Behúlová, and Martin Kotian

Slovak University of Technology in Bratislava, Ulica Jána Bottu č. 2781/25, 917 24 Trnava, Slovakia

The presented article focuses on the analysis of the results of laser welding simulation performed using the Design of Experiments (DOE) methodology. The aim was to evaluate the influence of selected characteristics of the conical heat source model on the shape (dimensions) and quality of the weld pool. A fully factorial design of type 2^3 was used for the design of the simulation experiments, which allowed to investigate not only the main effects of the three input factors: laser power (P), upper base radius (re) and lower base radius (ri), but also their possible interactions. The repetitions necessary for statistical processing of the results were obtained from simulations at the center point of the selected experimental area.

Numerical simulations were performed in the ANSYS 18.2 program using the 3D element SOLID70 using a conical volume model of the heat source with a Gaussian heat distribution. The input parameters ranged from P = 1200-1500 W, P = 0.3-0.7 mm and P = 0.3-0.5 mm. The output responses included the weld pool width and the molten zone density, which are considered critical for the weld quality.

Statistical analysis of the simulation results showed that the interaction effects of the selected parameters on the observed weld pool width response were not significant and could therefore be excluded from further consideration. All factors examined significantly affected the weld pool width, with laser power (P) and upper base radius (re) having a positive effect, while lower base radius (ri) showing a negative effect.

Regarding the molten zone density, laser power (P), lower base radius (ri) and the interaction of lower and upper base radius factors (ri*re) were identified as significant factors. The laser power (P) shows a significant positive effect. The effect of the lower base radius (ri) factor on the density of the molten zone is negative and is smaller than the laser power (P). The effect of the interaction of the base radius (ri*re) is comparable to the effect of the lower base radius (ri). Although the positive effect of the upper base radius (re) on the response to the density of the molten zone according to the results of the statistical analysis is not significant, due to the hierarchy of the regression model it was retained in the model. The center point was also included in the model due to the required curvature.

The developed regression models achieved high significance and accuracy, no lack of fit and high correlations with high R^2 values, which indicates their suitability for predicting the values of the studied weld characteristics.

This article presents a DOE-based approach for numerical simulations of laser welding and provides recommendations for the selection of geometric parameters of the heat source and laser power in order to optimize the weld quality.

Structure and properties of silver phosphate glasses with tungsten trioxide

Ladislav Koudelka, Tomáš Hostinský, and Petr Mošner

University of Pardubice, Faculty of Chemical Technology, Studentska 95, 532 10 Pardubice, Czech Republic

Phosphate glasses of the ternary system $Ag_2O-WO_3-P_2O_5$ were prepared and studied. Altogether 22 glass compositions were prepared and studied in five compositional series: (A) $40Ag_2O-xWO_3-(60-x)P_2O_5$, (B): $(60-y)Ag_2O-yWO_3-40P_2O_5$, (C) $zAg_2O-20WO_3-(60-z)P_2O_5$, (D): $50Ag_2O-kWO_3-(50-k)P_2O_5$ and (E) $30Ag_2O-nWO_3-(70-n)P_2O_5$. Basic physical parameters of glasses (density, molar volume, glass transition temperature, dilatometric softening temperature and the coefficient of thermal expansion) were determined. Glass transition temperature increases in the series A, D, E with increasing WO_3 content, nevertheless the highest value of $T_g = 500^{\circ}C$ was reached for the glass of the composition $10Ag_2O-50WO_3-40P_2O_5$ in the series B. Glass structure was studied by Raman spectroscopy and ^{31}P MAS NMR spectroscopy. In the studied ternary system glass forming region was determined and glasses with only $10 \text{ mol}\% P_2O_5$ were successfully prepared. The highest content of Ag_2O in these ternary glasses was 60 mol%. ^{31}P MAS NMR spectra revealed in the series (B): $(60-y)Ag_2O-yWO_3-40P_2O_5$ that with decreasing content of Ag^+ ions the number of nonbridging oxygen atoms decreases, while the number of W-O-P bridges in the structure increases.

Both Raman and NMR spectra revealed that with increasing WO_3 content in the studied glasses the depolymerization of the phosphate network takes place and the glass network is changed to tungstate-phosphate network, in which isolated PO_4 units are incorporated into the disordered tungstate network by W-O-P bonds. Tungsten atoms form WO_6 octahedra only and with increasing WO_3 content isolated WO_6 octahedra form chains or even clusters of tungstate units by W-O-W bridges.

A review of nucleation models in various systems

Zdeněk Kožíšek, Robert Král, and Petra Zemenová

Institute of Physics of the Czech Academy of Sciences, Cukrovarnická 10, 162 00 Praha 6, Czechia

Classical nucleation theory (CNT), which was originally derived for the formation of droplets, is often used to calculate the number of nuclei formed within a supersaturated or undercooled parent phase in various systems [1]. In some cases, however, the assumptions of CNT are not met, which is why the CNT approach is incorrect. Here, we summarize homogeneous and heterogeneous nucleation for vapor-liquid, vapor-solid, and liquid-solid phase transitions. In all cases, the formation of clusters plays an important role in the nucleation process. Nuclei of a new phase (supercritical clusters) form after overcoming the nucleation barrier W* at the critical size i*. In binary nucleation, W* corresponds to the saddle point when W reaches a minimum during the formation of nuclei. For heterogeneous nucleation on a foreign surface, W is influenced not only by interfacial energies but also by surface shape. A special case of heterogeneous nucleation is nucleation on active centers, where the nucleation barrier is lower, thus making active centers preferred for nucleation.

However, the formation of nuclei also depends on kinetics. In small encapsulated systems, the depletion of the parent phase, i. e., a decrease in supersaturation or a decrease in the number of atoms in the parent phase, influences the formation of nuclei. In very small systems, there is an insufficient number of monomers, so new nuclei cannot form. In the case of nucleation in a supersaturated vapor or solution within an encapsulated system, a decrease in supersaturation increases W, which influences the formation of nuclei.

For example, the polymorphic system L-glutamic acid (L-Glu) has two monotropic polymorphs: α -L-Glu (metastable) and β -L-Glu (stable). The numerical solution of the standard nucleation model [2] showed that the metastable α phase forms quickly. However, over time, the stable β phase forms and the metastable α phase disappears, which coincides with the Ostwald ripening mechanism.

Molecular dynamics (MD) simulations only allow us to simulate only limited time scales. However, the standard nucleation model overcomes this limitation, and the nucleation rates often coincide with MD simulations and experimental data [3].

- [1] D. Kashchiev, *Nucleation basic theory with applications*, Butterworth Heinemann: Oxford; Boston, 2000.
- [2] Y. Tahri, Z. Kožíšek, E. Gagnière, E. Chabanon, T. Bounahmidi, D. Mangin, *Modeling the Competition between Polymorphic Phases: Highlights on the Eect of Ostwald Ripening*, Cryst. Growth Des. 19 (2019) 3329.
- [3] L. G. V. Gonçalves, J. P. B. de Souza, E. D. Zanotto, *Assessment of the classical nucleation theory in supercooled nickel by molecular dynamics*, Mater. Chem. Phys. 272 (2021) 125011.

Laser performance overview of rare-earth doped multicomponent garnet crystal $Gd_3(Ga,Al)_5O_{12}$

<u>Jan Kratochvíl</u>¹, Pavel Boháček², Dominika Popelová¹, Jan Šulc¹, Michal Němec¹, Helena Jelínková¹, Bohumil Trunda², Lubomír Havlák², Karel Jurek³, and Martin Nikl³

¹Czech Technical University in Prague, Faculty of Nuclear Sciences and Physical Engineering, Břehová 78/7, Prague, 115 19, Czech Republic

²Institute of Physics of the Czech Academy of Sciences, Division of Condensed Matter Physics, Na Slovance 1999/2, 182 21 Prague 8, Czech Republic

³Institute of Physics of the Czech Academy of Sciences, Division of Solid State Physics, Cukrovarnická 10,162 53 Prague 6, Czech Republic

Crystaline multicomponent garnet Gd₃(Ga,Al)₅O₁₂ (GGAG) was investigated as a solid-state laser host material doped with trivalent rare-earth ions (RE³⁺). The use of this material as a laser active medium follows successful growth and investigation of Ce³⁺-doped GGAG as a high yield scintillator with good optical quality [1]. Several factors make the RE³⁺doped GGAG a promising active medium for diode-pumped, wavelength-tunable lasers. The crystal internal disorder and multi-site structure induces broadening of the dopant spectral lines. Wide absorption bands significantly decrease sensitivity to pump diode wavelength fluctuation. Broadening of emission lines contributes to obtaining broad and continuous wavelength tuning curve. The garnet structure offers advantages such as excellent thermal conductivity, considerable hardness and high damage threshold [2]. Spectroscopic and laser properties were investigated for GGAG doped with active ions such as Er³⁺, Yb³⁺, Pr³⁺, Tm³⁺, or Ho³⁺ [3-5]. This contribution focuses on spectroscopy and solid-state lasers based on Tm³⁺ and Ho³⁺ doped GGAG, emitting in 2 µm region. Compared to crystalline Tm:YAG, the Tm:GGAG absorption lines useful for diode pumping are broadened from $\Delta\lambda$ = 4 nm to $\Delta\lambda$ = 11 nm in the 0.8 µm region and from $\Delta \lambda$ = 15 nm to $\Delta \lambda$ = 35 nm near 1.7 µm, expressed as full width at half maximum (FWHM). Smooth laser emission wavelength tuning was obtained in range of 1870-2057 nm for Tm:GGAG and 1933-2118 nm for Tm, Ho: GGAG. Furthermore, watt-level continuous-wave operation was achieved under resonant diode pumping.

- [1] Yoshikawa, et al., Crystal growth and scintillation properties of multi-component oxide single crystals: Ce:GGAG and Ce:La-GPS, J. Lumin. 169, 387–393 (2016).
- [2] Kalisky, Y., The Physics and Engineering of Solid State Lasers, SPIE, 1000 20th Street, Bellingham, WA 98227-0010 USA (2006).
- [3] Švejkar, R. et al., Line-tunable Er:GGAG laser, Opt. Lett. 43(14), 3309 (2018).
- [4] Stehlík, M. et al., Wavelength tunability of laser based on Yb-doped GGAG crystal, Laser Phys. 28(10), 105802 (2018).
- [5] Kratochvíl, J., et al. Tm:GGAG disordered garnet crystal for 2 μ m diode-pumped solid-state laser, Laser Phys. Lett. 18(11), 115802 (2021).

Red-emitting Li₂MnCl₄ for neutron detection: crystal growth and new doping strategies

<u>Kateřina Křehlíková</u>^{1,2}, Vojtěch Vaněček¹, Robert Král¹, Petr Průša^{1,3}, Romana Kučerková¹, Vladimir Babin¹, Petra Zemenová¹, Jan Rohlíček¹, Kateřina Rubešová², and Martin Nikl¹

Scintillators are energy converters of ionizing radiation into photons in the visible, UV, and even IR regions. These emitted photons are detected by photodetectors (e.g., photomultiplier tube (PMT) or silicon-based photodetectors) and transformed into photoelectrons by multiplying the initial weak signal, which can be recorded with software [1,2]. The scintillator together with the photodetector form the scintillation detector.

Nowadays, neutron scintillators have their emission spectrum usually optimized for PMTs, for whose optimum wavelength in near UV-blue spectral region is demanded. However, in the field of neutronography, silicon-based photodetectors are desirable. Silicon-based photodetectors (charge-coupled device (CCD), thin-film transistor (TFT), avalanche photodiode (APD)) are generally less bulky, lighter, and cheaper than PMTs, they operate at lower voltages, and their maximum quantum efficiency is highest in the range of wavelengths above 500 nm. Therefore, a scintillator for thermal neutron detection based on reaction 6 Li(n, α) 3 H with emission in longer wavelengths would be optimal for silicon-based photodetector. Such a scintillator has not been under intensive development so far.

In our previous work, we introduced a novel red-emitting scintillator Li_2MnCl_4 , with high lithium content (28.5 at%), low density ($\varrho = 2.4 \text{ g/cm}^3$), low effective atomic number ($Z_{eff} = 17.1$) and emission in the red-NIR region [3]. These characteristics make Li_2MnCl_4 a promising candidate for measurements in high-flux mixed neutron-gamma fields. Moreover, the red-NIR emission is favorable for modern semiconductor photodetectors. The luminescence properties of Li_2MnCl_4 influenced by concentration quenching in the Mn^{2+} sublattice and further shaped by doping with Eu^{2+} and Ce^{3+} were also described.

In this work, we would like to follow up on the previous research by studying dopants with emission in longer wavelengths, such as Sm^{2+} , Ti^{3+} or In^+ .

- [1] Cieślak et al., Crystals, 9 (2019) 480.
- [2] Nikl et al., Advanced Optical Materials, 3 (2015) 463.
- [3] Vaněček et al., Materials Advances, 5 (2024) 8199.

¹Institute of Physics of the Czech Academy of Sciences, Cukrovarnická 112/10, 162 00 Praha 6, Czechia

²Faculty of Chemical Technology, University of Chemistry and Technology, Technicka 5, 166 28

Prague, Czechia

³Faculty of Nuclear Sciences and Physical Engineering, Czech Technical University in Prague, Brehova 7, 115 19 Prague, Czechia

Design and optimization of a rotating sample holder for high-temperature ion implantation

Matej Kubiš¹, Martin Cesnek², Martin Ševeček², and Pavol Noga¹

¹Slovak University of Technology in Bratislava, Faculty of Materials Science and Technology in Trnava, Ulica Jána Bottu č. 2781/25, 917 24 Trnava, Slovakia

²Czech Technical University in Prague, Faculty of Nuclear Sciences and Physical Engineering, Břehová 7, 115 19 Prague 1, Czech Republic

Accident Tolerant Fuels (ATF) are being developed to enhance the safety and resilience of nuclear fuel systems under severe accident conditions. These materials aim to overcome the limitations of conventional zirconium-based cladding, as highlighted by incidents such as the Fukushima Daiichi accident. Many ATF concepts involve modified cladding materials, such as surface coatings, composite structures, or alternative alloys.

Ion irradiation studies are commonly performed on flat samples due to experimental simplicity, however, this geometry fails to replicate the cylindrical structure, stress states, and thermal characteristics of actual fuel cladding. To enable more representative testing, we developed a rotating sample holder system for controlled ion implantation into tubular cladding samples at elevated temperatures.

A beam-shaping aperture was integrated into the design to prevent sputtering and change of the penetration depth at the sample edges. This aperture selectively masks portions of the ion beam, limiting sample exposure to the effective implantation area while covering the sample edges.

SRIM (The Stopping and Range of Ions in Matter) [1] and TRIDYN simulations were performed to model the ion implantation process and optimize the system parameters. The simulations provided data on the ion range distribution and at the selected energy to ensure penetration of the ions to the desired depth. We also obtained sputtering and strain information used to determine the aperture slit size.

[1] Ziegler, J. F., Ziegler, M. D., & Biersack, J. P. (2010). SRIM – The stopping and range of ions in matter (2010). Nuclear Instruments and Methods in Physics Research Section B: Beam Interactions with Materials and Atoms, 268(11–12), 1818–1823. https://doi.org/10.1016/j.nimb.2010.02.091

Statistical evaluation of metal plated polymer surfaces

Milena Kubišová¹, Barbora Lubdrovcová², Jana Knedlová¹, and Dagmar Endlerová¹

The surface quality of metallized polymer parts plays a crucial role in the functional and aesthetic properties of the final product, especially in the automotive industry and consumer electronics. This study focuses on non-contact measurement of the surface structure of ABS polymer parts, metallized using vacuum technology with the application of copper, nickel and chromium layers. The measurement was performed on the Talysurf CLI 500 device and evaluated according to the current standards ČSN EN ISO 21920-1 and 21920-2, which define the profile roughness parameters and the methodology for their assessment. The measured data were subsequently analyzed using descriptive statistics and multivariate statistical methods including analysis of variance (ANOVA), which allowed to reveal differences between samples manufactured in different time periods and in different plating conditions. The results confirm that the metal coating significantly affects the values of key surface structure parameters (Ra, Rz), and indicate the need for consistent control of process stability. The study also confirms the benefits of statistical tools for quality assessment and supports their wider use in technological practice.

¹Department of Production Engineering, Faculty of Technology, Tomas Bata Univerzity in Zlín, Vavrečkova 5669, 760 01 Zlín, Czech Republic

²Slovak Technical University in Bratislava, Faculty of Materials Technology based in Trnava, Institute of Production Technologies, Jána Bottu 8857/25 Trnava, Slovak Republic

Transparent Wood as a Sustainable Material for Photovoltaic Applications

Alexandra Kucmanová, Margita Ščasná, and Maroš Sirotiak

Slovak University of Technology Bratislava, Institute of Integrated Safety, Faculty of Materials Science and Technology, Botanická 49, 917 24 Trnava, Slovakia

Energy plays a key role in economic growth and development. As the population and economy grow, the energy demand also grows, and in the context of the climate crisis, renewable energy sources in particular are gaining increasing importance. Solar energy transformed through photovoltaic cells has become one of the main renewable sources. Research, development and production of photovoltaic cells have made enormous progress in recent decades. Investments are focused not only on increasing efficiency through new materials, but also on the ecological recycling of cells after their end of life. The production of traditional photovoltaic cells mainly uses high-purity monocrystalline and polycrystalline semiconductors (silicon, gallium arsenide, silver, germanium, indium, selenium, tellurium), glass and plastics for cell protection or perovskite for the production of low-cost photovoltaic cells, and aluminium for the production of cell frames. On the other hand, they also have disadvantages, such as e.g. fragility and high thermal conductivity in the case of glass, lower stability at higher temperatures, toxicity (presence of heavy metals such as lead, cadmium, bismuth, arsenic), shorter lifetime in the case of perovskite, and sustainable and ecological disposal and recycling of photovoltaic cells remains problematic.

For the above reasons, manufacturers and scientists are focusing on new, more stable and ecological materials. One of the most promising is transparent wood, which is produced by chemically removing lignin and other components from natural wood fibres and their subsequent impregnation with a transparent polymer (Epoxy, MMA, PMMA, PVP, PVA, etc.). The result is a material with excellent optical properties and mechanical strength, light, tough, with low density and thermal conductivity. Transparent wood is used in construction, for example, in window production, as a light-transmitting material for energy-efficient buildings (smart windows, roofs), as well as in modern architecture (interior and exterior design elements). However, due to its combination of transparency (up to 90%) and thermal insulation properties ($\lambda = 0.03$ to 0.07 W m⁻¹ K⁻¹), it is also of particular interest for the production of solar panels. It replaces traditional silica glass as a more economical and environmentally friendly alternative. Compared to conventional silicon solar cells, which require energy-intensive production processes, transparent wood has a significantly lower carbon footprint (silicon photovoltaic cells: transparent wood = 25 to 60 g CO₂e/kWh: 5 to 12 g CO₂e/kWh). Its renewable origin and lower environmental impact make it an eco-friendly and sustainable choice for widespread use in solar technologies.

Reliability of multi-state repairable systems

Eva Labašová and Vladimír Labaš

Slovak University of Technology in Bratislava, Faculty of Materials Science and Technology in Trnava, Ulica Jána Bottu č. 2781/25, 917 24 Trnava, Slovakia

The paper deals with the instantaneous and asymptotic availability and also the instantaneous and asymptotic unavailability of repairable multi-state systems [1]. Availability is understood as the ability of the system to be in a state capable of performing the required functions under given conditions, at a given time, provided that all required external resources are provided. Dynamic systems can be in different states at different times. These system states encompass properties such as functional, non-functional, partially functional, or partially non-functional, etc.

In the text of the contribution we will limit ourselves to the so-called homogeneous (or stationary) Markov processes, which are a suitable tool for analyzing the reliability of repairable technical systems [2]. We assume that both the operation and renewal intervals follow an exponential probability distribution.

The aim of the paper is to determine the asymptotic availability (and unavailability) of the system on a model example. Kolmogorov differential equations were used to determine them [3]. The availability of the system with increasing time is a decreasing function of time and the unavailability is an increasing function of time, but unlike the unrepaired system, their values stabilize at constant non-zero values. The paper presents possible ways to determine the steady availability and unavailability of the system on a model example.

- [1] Dhilon B S 2005 Reliability, Quality, and Safety for Engineers (CRC Press, USA)
- [2] Holub R and Vintr Z 2001 Reliability of aircraft engineering (VUT FSI, ČR)
- [3] Rausand M 2014 Reliability of Safety-Critical Systems: Theory and Applications (Wiley, USA)

Development and Application of HAXPES at TPS

Yen-Fa Liao

National Synchrotron Radiation Research Center, 101 Hsin-Ann Road, Hsinchu Science Park, 300092, Hsinchu, Taiwan

We have established a new Hard X-ray Photoelectron Spectroscopy (HAXPES) experimental end station at the Taiwan Photon Source (TPS) 47A beamline. This end station leverages the superior synchrotron radiation produced by the high-brightness TPS source and a high-energy-resolution monochromator (HRM) specifically designed for the 47A beamline. The TPS 47A beamline delivers outstanding performance, featuring an energy resolution below 100 meV and a photon flux exceeding 1×10^{11} photons/second. The beam spot size in our setup is approximately 6×6 microns.

Our HAXPES end station incorporates a modular chamber design that allows seamless switching between near-ambient pressure (NAP) and ultra-high vacuum (UHV) modes, enabling flexibility to accommodate various experimental needs. The high penetration depth of hard X-rays provides significant advantages for investigating semiconductor devices and multilayer systems, particularly when probing buried interfaces and inner layers.

A primary research objective of this end station is to study interfacial properties in semiconductor devices, with the aim of enhancing their efficiency and operational stability. HAXPES enables the detection of elemental distributions and chemical shifts at interfaces, providing insights into factors that influence device performance. These data are crucial for identifying degradation mechanisms and guiding device optimization. Furthermore, the development of in situ and operando measurement capabilities will be a key focus of ongoing research efforts at the HAXPES end station.

Application of finite difference method in solving phase-field models

Tereza Machajdíková and Roman Čička

Slovak University of Technology in Bratislava, Faculty of Materials Science and Technology in Trnava, Ulica Jána Bottu č. 2781/25, 917 24 Trnava, Slovakia

Phase-field modeling is a powerful tool in computational materials science, providing a useful framework for simulating microstructural evolution across various temporal and spatial scales. Unlike traditional sharp-interface approaches, phase-field modeling employs one or more continuous order parameters, or field variables, that vary smoothly across diffuse phase boundaries, thus eliminating the need to explicitly track interface positions. The phase-field model is valuable for simulating complex phenomena at the solder-substrate interface, particularly for implicitly tracking and predicting the growth and morphology of intermetallic compounds (IMCs), which are critical for understanding and optimizing solder joint reliability. In Phase-field model there are two main equations which drive this microstructural evolution: Allen-Cahn equation and Cahn-Hilliard equation. To numerically solve these complex phase-field equations, which are typically in the form of partial differential equations (PDEs), the Finite Difference Method (FDM) is applied. FDM approximates derivatives by finite differences on a discretized grid, transforming the continuous domain into a set of algebraic equations. The spatial derivatives in the governing equations are replaced by their finite difference approximations, converting the PDEs into a system of algebraic equations for the field variables at discrete grid points, which are then solved using numerical techniques to determine the approximate values of the field variables across the domain at each time step. In this work we present the numerical solution of phase-field model using finite difference method, specifically demonstrating its application to accurately simulate the complex intermetallic compound growth at the solder-substrate interface.

- [1] Biner, S. B., Programming Phase-Field Modeling. Springer Cham (2017)
- [2] Bellemans, I., Moelans, N. and Verbeken, K., Crit. Rev. Solid State Mater. Sci. 43 (2017) 417
- [3] Zhou, P. b., Electr. Energy Syst. Eng. Ser. (1993), Chap. 3
- [4] Mattiussi, C., Adv. Imag. Elec. Phys., 113 (2000) 1–146

Evaluation of the Physico-Mechanical Properties of ABS Polymer for Automotive Applications

Lenka Markovičová, Viera Zatkalíková, and Milan Uhríčik

University of Žilina, Univerzitná 8215/1, 010 26 Žilina, Slovakia

This article presents an evaluation of the physico-mehcanical properties of ABS ()Acrylonitrile Butadiene Styrene) polymer, specifically the Terluran HH 112 BK grade, used in the production of instrument panel covers in the automotive industry. The study was motivated by observed dimensional inaccuracies of the part during final assembly, which prompted a detailed investigation into potential material-related causes. A series of laboratory experiments were conducted to assess the material's properties and compare them with values provided in the manufacturer's datasheet. The results revealed deviations in mechanical prformancee, particulary in stiffness and dimension stability, which were further influenced by conditions during transport to the final assembly plant. The study identifies key factors contributing to product deformation and provides recommendations for improving the reliability of polymer components under real-world automotive conditions.

Influence of welding parameters on the microstructure and properties of laser welds of duplex steels

Maroš Martinkovič, Pavel Kovačócy, and Beáta Šimeková

Slovak University of Technology in Bratislava, Faculty of Materials Science and Technology in Trnava, Ulica Jána Bottu č. 2781/25, 917 24 Trnava, Slovakia

Duplex stainless steels are dual-phase alloys consisting of austenitic and ferritic phases in the microstructure which provide an ideal compromise between mechanical properties and corrosion resistance. Welding of DSS leads to a change of the microstructure and properties in weld joints. An innovative method of laser welding applying a dual beam was used. By spreading the energy of the laser beam over two spots, additional heat is introduced into the weld, which ensures a slowdown in the cooling rate during the welding process. The influence of laser focussing to microstructure and mechanical properties of the weld joints was monitored. Energy distribution of the dual beam was 50:50, total weld energy was constant. Using quantitative metallography ferrite/austenite ratio in fusion zone was determined. Mechanical properties of the welded joint were characterized by determination of shear strength and by the toughness in a fusion zone. For exact determination of the maximum value of the pressure force sensor must be calibrated.

Study of the effect of plate thickness on spatial resolution in novel optical guiding crystal scintillator

<u>Yuhei Nakata</u>^{1,2}, Kei Kamada^{2,3,4}, Tetsuo Kudo⁵, Masao Yoshino², Yasuyuki Usuki⁴, Naveenkarthik Murugesan^{1,2}, Kyoung Jin Kim³, Yuui Yokota², Syunsuke Kurosawa³, Hiroki Sato³, Takashi Hanada², Rikito Murakami², Akihiro Yamaji³, Satoshi Ishizawa², and Akira Yoshikawa^{2,3,4}

Scintillators, which convert radiation into visible light, are widely utilized in various fields, including medical diagnostics and non-destructive testing of industrial products. In X-ray imaging applications, achieving high resolution and sensitivity simultaneously is essential for obtaining clear images with short exposure times. However, conventional scintillator materials typically exhibit a trade-off relationship between resolution and sensitivity. To overcomes this issue, our research group previously proposed the use of structured scintillators, which can achieve both high resolution and high sensitivity. These are $GdAlO_3/\alpha$ - Al_2O_3 eutectic composites utilizing total internal reflection [1, 2] and optical-guiding crystal scintillators (OCS) [3-5]. The OCS consists of a low-refractive-index glass cladding and a high-refractive-index scintillator core, where scintillation light is guided like optical fibers through total internal reflection. This configuration facilitates the concurrent attainment of high resolution and high sensitivity by refining the core diameter and increasing the plate thickness.

This study employed Tl-doped $Cs_3Cu_2I_5$ scintillators as the core material and fabricated OCS plates ranging from 200 μ m to 800 μ m thick. These OCS plates, with 1 and 4 μ m core diameters and a 5 \times 5 mm² active area, were successfully fabricated. X-ray transmission images of resolution test charts were acquired using these OCS plates, along with commercially available Tl:CsI whiskers. The contrast transfer function (CTF) was then calculated for each line width to assess spatial resolution. The fabricated OCS plates exhibited higher light yield and superior spatial resolution than the commercial Tl:CsI whiskers. Notably, at 10 lp/mm, the CTF values were 39% for the OCS plate versus 23% for the Tl:CsI whiskers, indicating significantly improved spatial resolution. This presentation will detail the fabrication process, EBSD analysis and correlation between OCS plate thickness and spatial resolution.

- [1] K. Kamada, et al., Jpn. J. Appl. Phys. 60 (2021) SBBK04
- [2] A. Yoshikawa, et al. J. Crystal Growth. 498 (2018) 170-178
- [3] R. Yajima, A. Yoshikawa, et al., Appl. Phys. Express 16 (2023) 025505
- [4] R. Yajima, A. Yoshikawa, et al., Ceramics International 49 (2023) 41259-41263
- [5] R. Yajima, A. Yoshikawa, et al., Jpn. J. Appl. Phys. 62 (2023) SC1064

¹Tohoku University, Graduation School of Engineering, 6-6, Aramaki Aza Aoba, Aoba-ku, Sendai, Miyagi, Japan

²Tohoku University, Institute for Materials Research, 2-1-1 Katahira, Aoba-ku, Sendai, Miyagi, Japan

³Tohoku University, New Industry Creation Hatchery Center, 6-6-10 Aramaki, Aoba-ku, Sendai, Miyaqi, Japan

⁴C&A corporation, 7F Ichibancho Square, 1-16-23 Ichibancho, Aoba-ku, Sendai, Miyagi, Japan ⁵Mirai-Imaging corporation, 1-24 Uchigomimayamachi, Iwaki, Fukushima, Japan

Drag finishing as a post-treatment process of increasing the cobalt content in cemented carbide after plasma polishing

Boris Pätoprstý, Tomáš Vopát, Martin Sahul, and Samuel Lenghart

Slovak University of Technology in Bratislava, Faculty of Materials Science and Technology in Trnava, Ulica Jána Bottu č. 2781/25, 917 24 Trnava, Slovakia

This study investigates the use of drag finishing as a post-treatment method for sintered carbide cutting inserts with the aim of increasing the cobalt content in the surface layer. Cutting inserts initially polished by plasma discharge polishing exhibited a significantly reduced cobalt concentration at the surface, which poses a challenge for subsequent PVD coating adhesion. To address this issue, drag finishing was performed using two different media: walnut shell granulate and a mixture of walnut shell granulate with silicon carbide (SiC). The experiments were conducted using a drag finishing device developed at the Faculty of Materials Science and Technology, Slovak University of Technology in Trnava. The primary objective was to restore the surface cobalt content to a level comparable to that of the bulk material. Surface cobalt content was analyzed using energy-dispersive X-ray spectroscopy (EDX) in a scanning electron microscope (SEM). The results confirmed that drag finishing enables a partial restoration of cobalt content in the surface layer.

Thermal Plasma for the Synthesis of Advanced Functional Nanomaterials

Jakub Pilař^{1,2}, Alan Mašláni¹, and Maksym Buryi¹

¹Institute of Plasma Physics of Czech Academy of Sciences, U Slovanky 2525/1a 182 00, Prague, Czech Republic

²Faculty of Electrical Engineering, Department of Physics, Prague, Czech Republic

Thermal plasma represents a powerful and flexible tool for a variety of applications, including waste decomposition, upcycling, secondary raw material production, modification and synthesis. Thanks to its extreme nature, thermal plasma generates highly reactive thermochemical environment that can facilitate conditions for transformations and reactions that can otherwise be difficult or impossible to achieve via conventional methods.

A wide range of materials can be processed and converted into high-value products, including (a) organic feedstocks (biomass, wood, textiles, polymers) and wastes (food waste, refuse-derived fuel, medical waste) or (b) inorganic compounds like metals and metal oxides (Fe_2O_3 , TiO_2 , SiO_2 , ZnO, etc.). Depending on the configuration, the material can be directly injected into the plasma zone inside the reactor or treated by the plasma jet as pre-deposited layers or films on a substrate to enable localized surface treatment.

In addition to synthesis gas (mostly formed by $H_2 + CO$), resulting products can include carbon-based nanostructures (functional soot or carbon black), metal and metal oxide nanoparticles, or hybrid nanomaterials with specific surface chemistry, morphology and properties (either optical, thermal or electronic). These materials show promise in a wide array of technological applications like catalysis (including photocatalysis), energy storage, semiconductors, supercapacitors, sensors, medical and environmental remediation. Moreover, flexibility of the plasma process allows for scalable production from surface treatment of components to tens or even hundreds of kilogram-scale syntheses of particulate nanomaterials. To assesss the structural, chemical and functional properties of the output products, a variety of advanced characterization techniques is employed. These include AFM, SEM, TEM, XRD, XPS, QMS, FTIR, PL or Raman spectroscopy.

This contribution presents an overview of the possibilities offered by thermal plasma technology for the design and synthesis of novel functional nanomaterials from diverse input sources, including waste streams. Several experimental configurations and application-specific case studies will be introduced, with an emphasis on process control, materials engineering, and the interdisciplinary potential of plasma-based synthesis.

Micro-pulling-down grown Tm, Ho: GSAG crystal as laser gain medium

<u>Dominika Popelová</u>¹, Jan Kratochvíl¹, Jan Šulc¹, Michal Němec¹, Jan Pejchal², Jan Havlíček^{2,3}, Helena Jelínková¹, and Martin Nikl²

¹Czech Technical University in Prague, Faculty of Nuclear Sciences and Physical Engineering, Břehová 7, 115 19 Prague 1, Czech Republic

²Institute of Physics AS CR, Division of Solid State Physics, Cukrovarnická 10, 162 53 Prague, Czech Republic

³Crytur, Ltd., Na Lukách 2283, 511 01 Turnov, Czech Republic

Gadolinium-scandium-aluminium garnet (GSAG) is a relatively less-known crystal, primarily studied for scintillator applications [1]. While GSAG has been used as a laser host matrix doped with neodymium or erbium ions [2,3], only a few reports exist on thulium and holmium doping for laser emission around 2-2.1 μ m [4], making this a still largely unexplored area. Lasers operating around this wavelength range are highly relevant for free-space optical communication, LIDAR, environmental gas sensing (e.g., CO_2 and H_2O detection), medical applications, and pumping of mid-infrared optical parametric oscillators.

Traditionally, GSAG crystals are grown by the Czochralski method, which, although effective, can be time-consuming and resource-intensive. Alternatively, the micro-pulling-down (μ -PD) method offers a cost-effective approach to crystal growth. This method enables rapid crystal growth with minimal basic material consumption, which reduces costs and facilitates fast screening of different material compositions [5].

In this work, we explored a Tm,Ho co-doped GSAG crystal grown by the μ -PD method as active laser medium for generation around the wavelength of 2.1 μ m. We investigated laser performance under pulsed excitation at both 0.8 μ m and 1.7 μ m, as well as continuous-wave excitation at 1.7 μ m. Special attention was given to the tunability of the laser emission wavelength. Successful laser generation was achieved with slope efficiency reaching up to 30%, and a wavelength tuning range up to 138 nm. Our results demonstrate that μ -PD grown Tm,Ho:GSAG crystal represents a promising gain medium for widely tunable 2.1 μ m lasers, highlighting the advantages of the μ -PD growth method for efficient and economical laser crystal fabrication.

- [1] O. Zapadlík et al., RSC Adv. 15 (2025) 2140–2151.
- [2] S. G. P. Strohmaier et al., Opt. Commun. 275 (2007) 170–172.
- [3] Y. Chen et al., J. Alloys Compd. 814 (2020) 152267.
- [4] J. Šulc et al., Conference on Lasers and Electro-Optics Europe & European Quantum Electronics Conference (2023) CA-P.7.
- [5] J. Pejchal et al., International Conference on Crystal Growth and Epitaxy (2023) 51.

Optical spectroscopy and surface properties of doped nanocrystalline ZnO thin films on interdigital electrodes

<u>Zdeněk Remeš</u>¹, Neda Neykova^{1,2}, Naini Jain², Rupendra Kumar Sharma¹, Jakub Holovský^{1,2}, Egor Ukraintsev², Jaroslav Kuliček², Bohuslav Rezek², and Hua Shu Hsu³

¹FZU - Institute of Physics of the Czech Academy of Sciences, Na Slovance 1999/2, 182 00 Praha 8, Czechia

²Faculty for Electrical Engineering, Czech Technical University in Prague, Technická 2, 166 27 Prague, Czechia

³National Pingtung University, Department of Applied Physics, Pintung, Taiwan

Zinc oxide (ZnO) is a low cost and environmentally friendly material with unique optical properties and a variety of nano and microstructures imposing challenges for energy conversion, scintillators, photocatalytic wastewater treatment, electrochemical energy storage, or sensing applications. In this work, the nominally undoped and Al doped nanocrystalline ZnO thin films were pulsed laser deposited (PLD) [1] on commercial interdigitated gold electrodes gold-based Interdigitated Electrodes (IDE) on a glass substrate and tested using photothermal deflection (PDS) and photocurrent (PCS) spectroscopy [2]. Surface properties were characterized by Correlative Probe and Electron Microscopy (CPEM), that integrates Atomic Force Microscopy (AFM) and Scanning Electron Microscopy (SEM) to perform simultaneous correlated measurements of the same sample region.

- [1] E. Horynová, O. Romanyuk, L. Horák, Z. Remeš, B. Conrad, A. Peter Amalathas, L. Landová, J. Houdková, P. Jiříček, T. Finsterle, and J. Holovský, Thin Solid Films 693, 137690 (2020)
- [2] Z. Remes, N. Neykova, N. Jain, R. K. Sharma, J. Holovsky, E. Ukraintsev, J. Micova, and H. S. Hsu, in NANOCON 2024 Conference Proceedings (TANGER Ltd., Ostrava, Czech Republic, EU, Orea Congress Hotel Brno, Czech Republic, EU, 2024), pp. 291–295.

Plasmonic absorption in metal-ZnO nanocomplexes.

Bohuslav Rezek, Vendula Hrnčířová, Muhammad Qamar, and Egor Ukraintsev

České vysoké učení technické v Praze, Fakulta elektrotechnická, Technická 2, Praha 6, 166 27, Czechia

Zinc oxide nanoparticles (ZnO) exhibit semiconductor, photocatalytic, antimicrobial, and piezoelectric properties, while metal nanoparticles (mNP) can exhibit localized surface plasmonic resonance (LSPR) in visible spectral range. Here we study integration of both materials into a hybrid system and how it affects the mNP-ZnO properties for possible practical applications from optoelectronics to photocatalysis or biosensing. We investigate optical absorption of aqueous colloidal mixtures composed of ZnO nanoparticles with 20 nm silver (AgNP; LSPR at 394 nm, close to the adsorption edge of ZnO at 370 nm) and gold (AuNPs; LSPR at 524 nm far from the adsorption edge of ZnO), using UV-Vis spectrophotometry and RF electric field simulations. The mixtures show that higher concetration of mNPs (>) gives rise to supressed plasmonic absorption in the presence of ZnO. It is a similar effect as observed and explained for mixtures of mNPs with nanodiamonds [1]. However, spectral shift and across various concentration ratios of mNP and ZnO was not observed. Numerical modeling indicates that ZnO (unlike nanodiamonds [1]) minimally impacts the plasmonic absorption itself, but it enhances the local electromagnetic field of both mNP via dielectric effects.

[1] V. Hrncirova et al., Diamond Relat. Mater. 154 (2025) 112211.

Measurement of Thermally Induced Depolarization in Flash-lamp Pumped Nd: YAG Laser Rod

<u>Adam Říha</u>¹, Helena Jelínková¹, Jan Šulc¹, David Vyhlídal¹, Karel Veselský¹, Kryštof Kadlec¹, and Karel Nejezchleb²

¹Czech Technical University in Prague, FNSPE, Department of Laser Physics and Photonics, Břehová 7, Prague 1, 115 19, Czech Republic ²Crytur, Ltd. Turnov, Na Lukách 2283, 511 01 Turnov, Czech Republic

Nd³⁺:YAG crystals are one of the most used crystals as the laser active medium of solid-state lasers. They first appeared in 1964 [1] and in the near infrared region at wavelength of 1064 nm quickly became popular due to their high output energy and wide range of applications, from industrial materials processing and medicine to scientific research [2-4]. One of the key factors affecting the performance and optical properties of Nd:YAG lasers is the growth orientation of the crystal influencing the specific application requirements. Two most used orientations include <100> and <111> [5]. Each of these orientations has its own specific properties and uses. For some medical applications (e.g. melanin spot or tattoo removal [6]), radiation in the green region of the spectrum, i.e. the second harmonic generation of the Nd: YAG laser with a wavelength of 532 nm, is used. An undesirable phenomenon for efficient conversion of radiation by a nonlinear crystal located directly in the laser cavity is the depolarization of the amplified radiation with each passage through the laser rod between the resonator mirrors. Even if the depolarization after a single pass is very weak, due to multiple passages of radiation inside the resonator before the laser radiation exits through an output coupler, the plane of polarization can be significantly twisted, or radiation can be even completely depolarized. From this point of view, it was found that a crystal with a <100> orientation can be more advantageous. Nevertheless, during the crystal growth this structure can be changed. For this reason, it is needed to have some experimental instrument for radiation depolarization measurement thanks to which these changes can be detected.

In this work, a method of depolarization effect measurement was suggested and was applied for investigation and comparison of the flashlamp pumped <111>- and <100>-oriented Nd:YAG laser rods (Nd $^{3+}$ concentration of 1.1 at. % Nd/Y) with the diameter of 9.5 mm and length of 105 mm with faces bevelled at $4^{\circ}/4^{\circ}$ angles with antireflection coatings for the wavelength of the generated radiation. Depolarization was measured using a LD pumped compact passively Q-switched Nd:YAP/Cr:YAG nanosecond laser delivering a polarized radiation at the wavelength of 1078 nm.

- [1] J. E. Geusic et al., Appl. Phys. Lett., vol. 4(10), p. 182-184, 1964.
- [2] K. Washio, Mater. Chem. and Phys., vol. 31(1), p. 57-66, 1992.
- [3] L. Zhengjia et al., Laser/Optoelectronics in Medicine, Berlin, Springer, p. 267-267, 1986.
- [4] M. K. A. A. Razab et al., J. of Radiat. Res. Appl. Sci., vol. 11(4), p. 393-402, 2018.
- [5] H. Tünnermann et al., Opt. Express, vol. 19(14), p. 12992-12999, 2011.
- [6] G. Pincelli et al., J. Lasers Med. Sci., vol. 13, p. e79, 2022.

Lutetium hafnates: From ceramics to OFZ-grown single crystals

<u>Kateřina Rubešová</u>¹, Herbert Kindl^{1,2}, Vít Jakeš¹, Jan Pejchal², Vítězslav Jarý², Tomáš Thoř¹, Romana Kučerková², Vladimír Babin², and Christo Guguschev³

¹Department of Inorganic Chemistry, University of Chemistry and Technology, Technická 5, Prague 6, 166 28, Czech Republic

²Institute of Physics of the Czech Academy of Sciences, Cukrovarnická 10, Prague 6, 162 00, Czech Republic

³Leibniz Institute for Crystal Growth, Max Born Str 2, D-12489 Berlin, Germany

Heavy metal oxides, having high enough effective atomic numbers, belong to a group of inorganic materials that can fulfil the requirements for scintillators used in detection of high-energy photon radiation. Taking into account the state-of-the-art in the scintillators research, lutetium hafnates remain one of the last few poorly researched oxide materials, in both intrinsic and activated (for example, by cerium) scintillation. Within the Lu_2O_3 -HfO2 phase equilibrium, a gradual change from the cubic bixbyite-type Lu_2O_3 structure, via the cubic defect fluorite-type or pyrochlore-type solid solutions to the cubic hafnia stabilized by trivalent lutetium can be observed. In any case, the Lu_2O_3 -HfO2 system is represented by a few stoichiometric phases, pyrochlore $Lu_2Hf_2O_7$ and delta-phase $Lu_4Hf_3O_{12}$ being the representatives. All described structures are characterized by a defect-based crystal structure, very high material density and very high melting point, the latter probably being the reason why these materials are not as explored as others.

In this work, we present the synthesis of ceramic rods of lutetium hafnium oxide, both undoped and doped by cerium ions, and their use at crystal growth by Optical Floating Zone (OFZ) technique. The ceramic rods were processed by multi-step vacuum assisted sintering starting from lutetia, hafnia and ceria. Even though the use of vacuum at temperatures around $1600\,^{\circ}\text{C}$ can ensure the reduction of cerium from Ce^{IV} to Ce^{III} , additional annealing in reducing atmosphere was also tested and its influence on the scintillation characteristics was established. Then, the rods were processed in an OFZ furnace producing single crystals. Because of the inherently low thermal conductivity of this defect-type oxide, we tested the use of either $\text{Lu}_2\text{Hf}_2\text{O}_7$ pyrochlore stoichiometry or $\text{Lu}_2\text{Hf}_3\text{O}_9$ congruent stoichiometry to see if cracking of the grown single crystals can be prevented.

The prepared ceramic samples and single crystals were characterized by the Raman spectroscopy and X-ray diffraction to evaluate the crystal structure. Within the rare-earth hafnates ($RE_2Hf_2O_7$) family, the Lu^{III}/Hf^{IV} ionic ratio predicts that the defect fluorite-type lattice is more stable; however, we detected that the observed crystal structure is also dependent on the synthesis route used. The radioluminescence spectra, as well as the absorption spectra were measured at room temperature and those of undoped and cerium-doped samples were compared. Additionally, photoluminescence (PL) excitation and emission spectra at both room temperature and a temperature of 10 K, together with corresponding PL decay kinetics, were collected to detect the allowed 5d-4f transition of Ce^{III} ions.

Isotherm Study of Metribuzin and Tebuconazole Adsorption on Various Carbonaceous Materials

Margita Ščasná, Alexandra Kucmanová, Maroš Sirotiak, Michal Hebnár, and Maroš Soldán

Slovak University of Technology in Bratislava, Institute of Integrated Safety, Faculty of Materials Science and Technology, Botanická 49, 917 24 Trnava, Slovakia

This study examines the sorption capacity of various carbonaceous materials for removing metribuzin and tebuconazole from water under equilibrium conditions. The tested sorbents comprise hydrochars prepared from municipal wastewater sludge at $200\,^{\circ}$ C, $220\,^{\circ}$ C, and $240\,^{\circ}$ C, as well as one hydrochar from microalgal biomass at $220\,^{\circ}$ C, and commercial activated carbon used as a reference. All hydrochars were produced via hydrothermal carbonization, a process that lasted three hours.

Sorption experiments were conducted in batch mode using 10 mg of sorbent and 5 mL of pesticide solution with initial concentrations ranging from 10 to 50 mg/L. After 24 hours of contact, equilibrium concentrations were measured by high-performance liquid chromatography (HPLC-UV, Agilent 1260) equipped with a C18 reversed-phase column. Experimental data were fitted to both the Freundlich and Langmuir isotherm models.

Isotherm parameters enabled a comparison of sorption efficiency across sorbents, considering feedstock type and processing temperature. Hydrochars showed distinct sorption behaviours influenced by both parameters. The results suggest that waste-derived carbon materials have potential as cost-effective options for removing pesticides from water.

Keywords: Adsorption, biochar, hydrochar, activated carbon, metribuzin, tebuconazole, isotherm modelling.

Comparative Study of Selected Decontamination Agents for Surface Decontamination of Radionuclides

Margita Ščasná, Maroš Sirotiak, Alexandra Kucmanová, Tatiana Valová, and Maroš Soldán

Slovak University of Technology in Bratislava, Institute of Integrated Safety, Faculty of Materials Science and Technology, Botanická 49, 917 24 Trnava, Slovakia

This study focuses on the experimental evaluation of three decontamination agents for removing surface contamination from metal materials. Following ISO 7503 standards, stainless steel test plates made of austenitic (AISI 304) and ferritic (AISI 430) steel, each measuring 5×5 cm and differing in surface roughness, were intentionally contaminated. The applied radionuclides included technetium-99m (99m TcO⁴⁻ and 99m Tc labeled human albumin nanocolloid) and iodine-123 (123 I-ioflupane), commonly used in nuclear medicine.

The tested decontamination agents were Incidin (an alcohol-based disinfectant), Neodekont with water (an abrasive dermocosmetic cleaning agent), and a 0.5% aqueous solution of citric acid. The experiment involved measuring surface activity before and after three decontamination cycles using both direct and indirect methods. Based on the measured values, decontamination efficiency and decontamination factors were calculated relative to the regulatory limits for environmental release and surface use in controlled workplaces.

Decontamination results varied depending on the type of radionuclide, surface finish, and the cleaning agent used. In several cases, the remaining activity fell below the regulatory threshold, which allowed the material to be reused or released. On smooth steel, contaminants were removed more easily -probably because the surface held less material and the cleaning agent spread more evenly. Rougher surfaces tended to have more contamination and often required multiple cleaning steps to reduce activity below acceptable limits.

These results underscore that decontamination effectiveness depends not only on the properties of the radionuclide and the agent chemistry, but also on the physical condition of the contaminated surface. Choosing an appropriate cleaning method requires consideration of all these factors. Calculated decontamination factors provided a more reliable basis for determining whether the cleaned surface met legal requirements compared to efficiency alone.

Keywords: austenitic steel, decontamination, decontamination factor, ferritic steel, radionuclides, surface contamination.

Structural, Morphological, and Optical Analysis of High-Purity ZnO Microrods

Shelja Sharma and Maksym Buryi

Institute of Plasma Physics of the Czech Academy of Sciences, U Slovanky 2525/1a 182 00, Prague 8, Czech Republic

Zinc oxide (ZnO) microrods were successfully synthesized using a hydrothermal method in an alkaline aqueous medium optimized for high purity and morphological uniformity. The resulting structures were characterized using scanning electron microscopy (SEM), energy-dispersive X-ray spectroscopy (EDS), X-ray diffraction (XRD), and Photoluminescence (PL) spectroscopy to comprehensively investigate their structural, morphological, and optical properties. SEM analysis revealed the formation of ZnO microrods with hexagonal cross-sections, suggesting well-controlled anisotropic growth. At low magnification, the microrods are seen to be uniformly distributed across the surface. At higher magnification, individual micro-rods exhibit well-defined hexagonal facets and smooth sidewalls, with diameters typically ranging from 1 to 2 μ m and lengths extending to several micrometers. These features highlight the high morphological uniformity and directional growth along the c-axis. Elemental analysis using EDS confirmed the high purity and near-stoichiometric composition of the ZnO microrods, with no detectable secondary phases. Structural analysis by XRD confirmed a singlephase hexagonal wurtzite structure, consistent with zincite. The sample exhibited sharp diffraction peaks with refined lattice parameters of a = 3.2511 Å, c = 5.2108 Å, and a crystallite size of 110 nm, indicating a polycrystalline origin of the individual microrods. The Raman and PL measurements provide complementary insights into its structural and optical properties. The Raman spectrum displays a prominent peak around 435 cm⁻¹, characteristic of ZnO's crystalline phonon modes such as E_2 and A_1 (TO), along with a broad background extending beyond 1000 cm⁻¹, suggesting the presence of structural defects or multi-phonon processes. The PL spectrum reveals a sharp but relatively weak UV emission around 380-390 nm, indicating near-band-edge excitonic recombination, while a several orders of magnitude stronger and broader visible white emission covering the range of 400-700 nm points to a high concentration of intrinsic defects like oxygen or zinc vacancies and interstitials. Along with the highly uniform rod-like morphology and good crystallinity, combining these rods with ultrafast cesium lead bromide having about 2.5 eV bandgap can result in the new generation of ultrafast scintillators engineering.

Analysis of Wire Electrode Wear in the WEDM Machining of Inconel 625

Vladimír Šimna

Slovak University of Technology in Bratislava, Faculty of Materials Science and Technology in Trnava, Ulica Jána Bottu č. 2781/25, 917 24 Trnava, Slovakia

The aim of this study was to analyze the influence of selected electrical parameters on the wear of coated wire electrodes during the wire electrical discharge machining (WEDM) of high-strength Inconel 625. The experiment was carried out using two types of 0.25 mm diameter electrodes: Elecut X (coated electrode with a copper core) and SuperZinc (coated electrode with a brass core, CuZn37). Electrode wear was determined by a gravimetric method, comparing the weight loss before and after the cutting process using Kern analytical scales with a resolution of 0,001 g.

The experimental parameters included pulse width (A), pulse interval (B), servo reference voltage (Aj), ignition pulse current (IAL), and short discharge duration (TAC). The parameters during machining were monitored using a KEYSIGHT EDUX1002A oscilloscope. The experiment was designed using the Taguchi method with an L27 orthogonal array, and the influence of individual factors on electrode wear was evaluated using analysis of variance (ANOVA).

The results confirmed a significant influence of certain electrical parameters on the rate of electrode wear, while the differences between the electrode types highlight the need for optimization of WEDM process settings depending on the electrode type.

Single Crystal Growth of Mg and Ce co-doped Y₃(Ga,Al)₅O₁₂ with various Mg concentration and their scintillation properties

<u>Hisato Suezumi</u>^{1,2}, Kei Kamada^{3,4}, Masao Yoshino^{2,3}, Kyoung Jin Kim³, Rikito Murakami^{2,3}, Satoshi Ishizawa^{2,3}, Akihiro Yamaji^{2,4}, Shunsuke Kurosawa⁴, Yuui Yokota^{2,4}, Hiroki Sato^{2,4}, Takashi Hanada², and Akira Yoshikawa^{2,3,4}

¹Graduation school of Engineering, Tohoku University, Japan
²Institute for Materials Research (IMR), Tohoku University, Japan
³C&A corporation, Japan
⁴ New Industry Creation Hatchery Center (NICHe), Japan

[Introduction] Ce:Gd₃(Ga,Al)₅O₁₂ (GAGG) single crystal has been attracted as scintillator in X-ray photon-counting detectors (PCDs) for Photon Counting Computed Tomography (PCCT) in the medical field. However, the K-absorption edge of Gd is at around 50 keV which is in the range of the X-ray inspection energy region, can affect to the degrade of imaging quality due to the difficulty in energy discrimination. On the other hand, Ce:Y₃(Ga,Al)₅O₁₂ (YAGG) single crystal has been focused on as a candidate material for PCDs scintillator since the K-edge of Y is at around 17 keV which is out of the X-ray energy region, therefore, it is possible to discriminate the energy well. On the other hands, the micro-pulling down (μ -PD) method^[2] based material explorations have been conducted in YAGG. Among them, Mg co-doped Ce:Y₃Ga_xAl_{5-x}O₁₂ (x=2,3) showed the higher light yield of 36,000-38,800 photons/MeV and shorter decay time of below 20 ns. This enhancement of light yield and decay time shortening are expected to be the effect of Mg²⁺ to the increase in conduction band minimum by changing the Ce charge from Ce³⁺ to Ce⁴⁺ states. However, the detailed luminescent properties related to co-doping with Mg and the presence of Ce⁴⁺ remain unresolved.

[Results and Discussion] In this research, Mg and Ce co-doped $Y_3Ga_xAl_{5-x}O_{12}$ single crystals were grown by the μ -PD method with various Mg concentrations. The scintillation properties and the effect of Mg²⁺ to the defects were measured. Single crystals of Mg,Ce: $Y_3Ga_xAl_{5-x}O_{12}(x=2,3)$ were grown with a radio frequency heating system. Yellow like colored single crystals with 3 mm diameter and 70 mm length were grown. Mg,Ce: $Y_3Ga_2Al_3O_{12}$ showed a light yield of 44,000 photons/MeV and decay time of 50 ns. For further investigation of the understanding of Mg co-doping effect on YAGG, optical absorption measurement and positron annihilation measurement were conducted. As the increase in Mg²⁺ concentration, Ce³⁺(4f-5d₁) absorption sharply decreased to 0, and the absorption intensity around 200-350 nm highly increased from the optical absorption spectra, and the previous defect engineering study in the Mg²⁺ co-doped Lu₃Al₅O₁₂ showed the same absorption phenomenon. Mg²⁺ concentration from the positron annihilation measurement. Therefore, the absorption enhancement of the charge transfer suggested an increase in Ce⁴⁺ is expected to be due to the charge compensation of Mg²⁺ which compensates for defects.

- [1] K. Shimazoe, et al. Communications Engineering 3.1 (2024): 167.
- [2] A. Yoshikawa et al., Opt. Mat. 30(1)(2007) 6-10.
- [3] K.Kamada, et al, IOP Conf. Ser.: Mater. Sci. Eng. 169 (2017) 012013.
- [4] K. Omuro, et al. Journal of Alloys and Compounds 1008 (2024): 176550.

Temperature dependence of internal damping of austenitic steel in different states

<u>Milan Uhríčik</u>, Peter Palček, Silvia Hudecová, Veronika Chvalníková, Martin Slezák, Edita Illichmanová, and Zuzana Šurdová

University of Žilina, Faculty of Mechanical Engineering, Department of Materials Engineering, Univerzitná 8215/1, 010 26 Žilina, Slovakia

There is currently considerable interest in the effective use of austenitic steels, especially in areas where high corrosion resistance, toughness and good mechanical properties at elevated and cryogenic temperatures are required. Austenitic steels, due to their face-centered cubic (FCC) lattice, exhibit exceptional plasticity and good damping properties. Their internal damping is closely related to microstructural factors such as the presence of dislocations, interaction with precipitates, work-induced martensitic transformation or dynamic rearrangement of dislocation structures [1, 2].

The primary mechanism of internal damping in austenitic steels is the interaction between moving dislocations and point or linear defects, with slip and mechanical twinning also playing a significant role. Cold working leads to an increase in the density of dislocations, which can temporarily increase the damping capacity of the material, but at the same time it can decrease at higher plastic deformations due to structural stabilization. Alloying elements such as Mn, Ni or Mo affect the stability of the austenite phase and thus indirectly the damping properties. The transformation of austenite to martensite under load can contribute to higher energy dissipation and thus better internal damping under certain conditions. [1, 2].

Internal damping is a very sensitive experimental method that allows for detailed investigation of structural defects and their dynamics in materials. This method provides valuable information about transport phenomena and solid-state phase transformations that are difficult to detect with other techniques. The measuring system consists of control and evaluation components as well as heating and ultrasonic parts. The ultrasonic generator generates a sinusoidal signal, which is then amplified and converted into mechanical waves using a piezoceramic transducer.

- [1] M. Oravcová, P. Palček, M. Chalupová, and M. Uhríčik, MATEC Web of Conf. 157 (2018).
- [2] T. Oršulová, P. Palček, M. Uhríčik, and M. Roszak, Trans. Res. Proc. 40 (2019) 68.

A brief introduction to Judd-Ofelt theory: Application to rare earth-doped silicate glass

<u>Petr Vařák</u>^{1,2}, Jan Hrabovský^{3,4}, Robin Kryštůfek^{5,6}, Artem Simoniakin¹, Pavla Nekvindová¹, Michal Kamrádek², and Pavel Peterka²

¹University of Chemistry & Technology, Prague, Technická 5, Praha 6, Czechia
 ²Institute of Photonics & Electronics of the CAS, Prague, Czech Republic
 ³Faculty of Mathematics and Physic, Charles University, Prague, Czech Republic
 ⁴Department of Physics, New Mexico State University, Las Cruces, NM, United States
 ⁵Institute of Organic Chemistry and Biochemistry of the CAS, Prague, Czech Republic
 ⁶Faculty of Science, Charles University, Prague, Czech Republic

Rare-earth (RE) elements and their trivalent ions remain highly relevant in both science and industry thanks to their unique electronic, magnetic, and optical properties, especially the sharp absorption and emission lines owing to the intra 4f-4f electron transitions.

The Judd-Ofelt (J-O) theory, introduced in 1962 by B. R. Judd and G. S. Ofelt, remains a staple in the analysis of the optical properties of the 4f-4f electronic transitions in trivalent rare earth ions [1, 2]. The J-O theory starts with the free ion Hamiltonian of a 4f electron, which has no exact solution, and using several approximations and assumptions, arrives to a simple expression for the so-called line strength, S, of each transition. The analysis under the umbrella of the J-O theory allows to use measured absorption cross sections to calculate the experimental values of line strengths, and using a simple least squares method, obtain three phenomenological J-O parameters, Ω_i , where i = 2, 4 and 6 [3]. The parameters are subsequently used to calculate the transition probabilities, branching ratios, radiative lifetimes and quantum efficiency - all crucial parameters in various theoretical tasks and simulations, e.g. the calculations of emission cross sections, energy transfer coefficients, etc., making the J-O analysis one of the most important tools of materials research in photonics.

In this contribution, the main concepts and background of the rare earth ion spectroscopy are summarized, and the J-O theory is briefly introduced. We introduce the newly developed, on-line and free-to-use software LOMS.cz [4]. The Spectroscopic properties of several glass systems are measured, and the J-O analysis is conducted using the LOMS.cz software. The utility and practical application of the J-O theory are demonstrated on the results.

- [1] B. R. Judd, 'Optical Absorption Intensities of Rare-Earth Ions', Phys. Rev., 1962
- [2] G. S. Ofelt, 'Intensities of Crystal Spectra of Rare-Earth Ions', J. Chem. Phys., 1962
- [3] B. M. Walsh, 'Judd-Ofelt theory: principles and practices', Springer Netherlands, 2006
- [4] J. Hrabovský, P. Vařák, and R. Kryštůfek, 'LOMS.cz: A computational platform for high-throughput Classical and Combinatorial Judd-Ofelt analysis and rare-earth spectroscopy', Scientific Reports 15, 28945, 2025. https://doi.org/10.1038/s41598-025-13620-0

Photo- and radioluminescence of willemite in ZnO-Al₂O₃-SiO₂ glass system

<u>Jakub Volf</u>¹, Petr Vařák^{1,2}, Vítězslav Jarý³, Vladimir Babin³, Emmanuel Véron⁴, Mathieu Allix⁴, and Pavla Nekvindová¹

In recent years, glass systems containing ZnO, Al_2O_3 , and SiO_2 as main components have been investigated for the possibility of developing glass-ceramics. In particular, technology for creation of nanocrystalline phases, which depends on chemical composition and heat treatment temperature, is being sought [1,2]. Research in the aforementioned glass system focuses mainly on gahnite (spinel $ZnAl_2O_4$) and willemite (rhombohedral Zn_2SiO_4), which are interesting for their use in optics and photonics. The willemite phase, especially, has been shown to exhibit interesting and strong radioluminescence [3].

Our contribution describes glass-melting processes, composition, microstructure and especially optical properties of a large set of samples. Melt-quenching method and aerodynamic levitation with laser heating were used to prepare the samples. Both methods used to prepare willemite glass ceramics were compared. Chemical composition and microstructure was checked by XRF, XRD, SEM or EDS. Absorption, photoluminescence and radioluminescence spectra were measured. The special attention is paid to relationships between composition, structure of the glasses/glass ceramics and used technology.

- [1] P. Vařák, J. Baborák, E. Véron, A. Michalcová, J. Volf, M. Allix, and P. Nekvindová, Journal of Non-Crystalline Solids, 626 (2024), 122783.
- [2] Y. Guo, C. Liu, J. Wang, J. Ruan, J. Xie, J. Han and X. Zhao, Journal of the European Ceramic Society, 42(2), 576-588.
- [3] V. Jarý, P. Vařák, J. Hrabovský, A. Michalcová, J. Volf and J. Mrázek, Optical Materials, 162 (2025), 116961.

¹Department of Inorganic Chemistry, University of Chemistry and Technology, Technická 5, 166 28, Prague, Czech Republic

²Institute of Photonics and Electronics of the Czech Academy of Sciences, Chaberská 1014/57, 182 51 Prague, Czech Republic

³FZU-Institute of Physics of the Czech Academy of Sciences, Cukrovarnická 10/112, 162 00 Prague 6 ⁴CEMHTI – CNRS UPR3079, 1 Av. de la Recherche Scientifique, 45100, Orléans, France

Influence of cutting tool geometry on machined surface roughness when machining thin-walled components from Inconel 718 manufactured by WAAM

Marek Vozár, Tomáš Vopát, and František Jurina

Slovak University of Technology in Bratislava, Faculty of Materials Science and Technology in Trnava, Ulica Jána Bottu č. 2781/25, 917 24 Trnava, Slovakia

This study investigates the influence of cutting tool macrogeometry on the surface roughness of thin-walled Inconel 718 components produced by Wire Arc Additive Manufacturing (WAAM). Several tools with varying geometrical features were tested with the goal of minimizing vibration during machining. However, some tool parameter configurations led to visible marks on the machined surface. Surface roughness was analyzed using focus variation microscopy, evaluating parameters such as Ra, Rz, and Rq to capture key surface characteristics. A comparison was made between the tool that demonstrated the lowest wear and the tool that achieved the best surface finish. The analysis revealed that while certain tool geometries reduced wear, they did not necessarily result in improved surface quality. Additionally, insufficient coolant delivery to the cutting zone was identified as a contributing factor to irregular surface patterns. The findings highlight the importance of carefully selecting tool geometry and optimizing process conditions when machining WAAM-produced thin-walled parts from Inconel 718.

All-inorganic perovskite quantum dots: a fundamental building block for optical neuromorphic synapse devices

Yung-Chi Yao¹ and Ya-Ju Lee¹,²

Here we present our recent advancements in the development of multifunctional optoelectronic devices based on allinorganic perovskite (CsPbBr₃) quantum dots (QDs). We first demonstrate a dual mode device capable of operating either as an optical sensor or as an artificial synapse, with its functionality determined by the applied electrical polarity [1, 2]. This represents a significant step toward the realization of the first homogeneously integrated synaptic device based on perovskite QDs. Our device offers direct evidence that colored image recognition and nearsensor computation can be achieved within a unified and compact architecture. In addition, we present a resonantly enhanced photodetector with builtin color selectivity, achieved via monolithic integration of CsPbBr₃ QDs into a Tamm plasmon (TP) structure [3, 4]. Due to its narrow spectral response, the proposed device exhibits synaptic dynamics, multilevel conductance modulation in response to repetitive light stimuli at the resonant wavelength, enabling key neuromorphic functions such as colordependent memory encoding and visual perception. These findings collectively represent a substantial advancement in neuromorphic computing platforms and open a new horizon for allinorganic perovskite optoelectronic technologies.

- [1] M.-C. Yen et. al., Nat. Comm, 12 (2021), 4460.
- [2] Y.-C. Yao et. al. Adv. Sci. 12 (2025) 2409933.
- [3] M.-C. Yen et. al. Adv. Opt. Mater. 11 (2023) 2202326.
- [4] M.-C. Yen et. al. Adv. Sci. (2025) e03464.

¹Program on Key Materials, National Cheng Kung University, No.1, University Road, 701, Taiwan ²Department of Photonics, National Cheng Kung University, No.1, University Road, 701, Taiwan

Influence of Ga/Al Ratio on Luminescence and Scintillation in Ce3+/Tb3+ Co-Doped Gd3(Ga,Al)5O12 Scintillators

Masao Yoshino¹, Kazuya Omuro¹, Karol Bartosiewicz², Liudmila Gushchina³, Takahiko Horiai⁴, Kyoung Jin Kim^{3,4}, Kei Kamada^{3,4}, Seiichi Yamamoto⁵, Kohei Nakanishi⁶, and Akira Yoshikawa^{1,3,4}

¹Tohoku University, Institute for Materials Research, Sendai, Miyagi, 980-8577, Japan

²Institute of Physics of the Czech Academy of Sciences, 18200 Praha, Czechia

³C&A Corporation, Sendai 980-8579, Miyagi, Japan.

⁴Tohoku University, New Industry Creation Hatchery Center, Sendai 980-8579, Miyagi, Japan.

⁵Waseda University, Faculty of Science and Engineering, Tokyo 169-8555, Japan

⁶Nagoya University, Graduate School of Medicine, Nagoya 461-8673, Japan.

In recent years, the integration of advanced X-ray imaging methodologies with monochromatic X-ray sources has enabled imaging at submicron to micron scales, thereby garnering significant interest in high-resolution synchrotron radiation X-ray imaging research [1]. Oxide single-crystal scintillators represent a critical class of functional materials distinguished by their high density, large effective atomic number, and superior physical and chemical stability—properties that render them particularly well-suited for X-ray imaging applications [2]. Among these materials, Ce³⁺-doped Gd₃(Ga,Al)₅O₁₂ (GGAG:Ce) exhibits the highest light yield reported to date among oxide-based single-crystal scintillators, positioning it as one of the most promising candidates for X-ray detection [3]. In recent investigations, we have focused on co-doping Ce³⁺ and Tb³⁺ ions within the garnet crystal structure. Co-doped Ce³⁺,Tb³⁺ scintillators have demonstrated enhanced luminescence and scintillation performance attributed to efficient energy transfer between the two ions [4]. Specifically, Ce³⁺ emission, originating from the 5d–4f transition, is highly sensitive to the crystal field due to the spatial extension of the 5d orbital. In contrast, Tb^{3+} emission, governed by 4f–4f transitions, is largely unaffected by crystal field variations due to the localization of 4f electrons near the nucleus. Consequently, while the luminescence characteristics of Ce³⁺ are influenced by the host composition, those of Tb³⁺ remain relatively stable.

In this study, we investigated the bidirectional energy transfer dynamics between Ce^{3+} and Tb^{3+} as a function of Ga-to-Al ratio (x=1,2,3,4) in $Gd_3Ga_xAl_{5-x}O_{12}$. Crystals with the composition $Gd_3Ga_xAl_{5-x}O_{12}$:0.5%Ce, 15%Tb (x=1,2,3,4) were grown using the micro-pulling-down method, and their photoluminescence, photoluminescence excitation, and radioluminescence characteristics were evaluated. The results revealed that the efficiency of bidirectional energy transfer between Ce^{3+} and Tb^{3+} was dependent on the Ga:Al ratio, with the highest total radioluminescence intensity observed at a Ga:Al ratio of 3:2. In addition to a discussion on luminescence behavior, this study also presents the successful growth of large single crystals via the Czochralski method and demonstrates their practical applicability through X-ray imaging experiments.

- [1] T. Martin, A. Koch, J. Synchrotron Radiat. 13 (2006) 180–194.
- [2] M. Nikl, A. Yoshikawa, Adv. Opt. Mater. 3 (2015) 463–481.
- [3] K. Kamada, and A. Yoshikawa et al., Cryst. Growth Des. 11 (2011) 4484–4490.
- [4] K. Omuro, M. Yoshino, and A. Yoshikawa et al., J. Lumin. 273 (2024) 120663.

Effect of long-term exposure to chloride-containing solution on degradation of plasma-nitrided layer on AISI 316L stainless steel

Viera Zatkalíková, Lenka Markovičová, Martin Slezák, Milan Uhríčik, and Martin Vicen

University of Žilina, Faculty of Mechanical Engineering, Department of Materials Engineering, Univerzitná 8215/1, 010 26 Žilina, Slovakia

Conventional plasma nitriding (PN) at temperatures above 500 °C (so called high-temperature plasma nitriding) is a common thermo-chemical treatment used to increase surface hardness and improve tribological properties of stainless steels. Due to the protective passive surface film stainless steels are generally highly corrosion resistant in oxidation environments, but in chloride-containing ones they are susceptible to the local pitting corrosion. Although these materials own a favorable combination corrosion resistance/adequate mechanical properties, without a special surface treatment they are not suitable as a construction materials for applications where high wear resistance is required.

At a PN temperature of approx. 500 - 550 °C, an intensive diffusion of nitrogen atoms into the surface layer and their reactions with chromium are thermodynamically favored and hard chromium nitrides are formed. On the one hand, the chromium nitrides precipitation brings a significant increase in hardness and wear resistance, on the other hand, due to chromium depletion, corrosion resistance is generally reduced. A worse quality of passive film or loss of passive behavior were recorded by numerous authors mostly by electrochemical measurements performed in various chloride solutions. Studies evaluating the resistance of conventionally plasma-nitrided stainless steels surface to degradation induced by long-term exposure to chloride-containing environments are lacking.

The main objective of this study is an assessment of the plasma-nitrided surface layer degradation during 2-month exposure of plasma-nitrided (530 °C, 24 hours) AISI 316L specimens to 0.5 M NaCl solution at room temperature (20 \pm 3 °C). Evaluation is based on corrosion rates calculated from the mass losses of the specimens during exposure and on the characterization of the plasma-nitrided layer before and after exposure (SEM, roughness, micro-hardness and potentiodynamic polarization performed in 0.5 NaCl solution at room temperature).

The experiment results point to an intensive corrosion degradation of the PN layer during exposure, proved by its lower thickness, decreased micro-hardness and by the changed surface roughness parameters. According to the potentiodynamic polarization parameters measured after exposure, degradation of the plasma-nitrided layer led to an improvement of corrosion behavior compared to the state before.

Design and Development of a Transfer Cassette for Air-Sensitive Hazardous Materials in High Vacuum Ion Beam Systems

Pavlína Zavadilová, Jozef Dobrovodský, Pavol Noga, and Zoltán Száraz

Slovak University of Technology in Bratislava, Faculty of Materials Science and Technology in Trnava, Ulica Jána Bottu č. 2781/25, 917 24 Trnava, Slovakia

High vacuum ion beam systems require specialised sample handling solutions for air-sensitive hazardous materials that degrade upon atmospheric exposure. Due to the absence of airlocks in our experimental facilities, we encountered the problem of sample transfer from glovebox to chamber and interchamber movement. Since there are no commercial products that are compatible with our equipment, we had to develop our own solution for sample transfer. Comprehensive design and development of a transfer cassette system fulfils both safety and analytical requirements for ToF-ERDA (Time-of-Flight Elastic Recoil Detection Analysis).

The cassette introduced in this work was designed using Fusion 360 CAD software, building upon existing ToF-ERDA sample holder geometry to ensure system compatibility. Key design requirements included: maintaining inert atmosphere during transfer, ensuring high vacuum material compatibility and providing universal use without sample-specific modifications, opening and closing mechanism without additional electrical leads.

Material and sealing elements were optimised for ultra-high vacuum compatibility while preventing atmospheric contamination. The optimisation process focused on balancing compact dimensions, opening and closing mechanisms.

The resulting design provides a universal cassette system for safe transferring air-sensitive hazardous materials to high vacuum ion beam systems without compromising measurement quality. This solution extends the possibilities of analysis to materials that degrade when exposed to air in the field of thin film lithium batteries, hydrogen storage and energy materials development.

Compositional analysis of NaCl by thermoanalytical, structural, and optical methods for controlled combustion of nanodiamond particles

<u>Petra Zemenová</u>, Alexandra Falvey, Vojtěch Vaněček, Aleš Bystřický, Štěpán Stehlík, and Robert Král

Institute of Physics of the Czech Academy of Sciences, Cukrovarnická 10, Prague 162 00, Czechia

Sodium chloride (NaCl) is one of the best known and most studied materials in the history of materials science. It has a wide range of applications from material's research, chemical industry, to common household use or as a material for sprinkling in winter. Interestingly, NaCl was recently also used as a catalyst for nanodiamond (ND) purification, rounding, and shape modifications; however, the origin of such an effect still remains unclear. This work is motivated to investigate the NaCl behavior deeper and reveal the cause, which could lead to such behavior.

In this work, the NaCl powder samples and a single crystal of NaCl were studied by thermal analyses such as differential scanning calorimetry (DSC) and thermogravimetry (TG), mass spectrometry (MS), optical stereomicroscopy (OM), optical thermomicroscopy (OTM), and powder X-ray diffraction (XRPD). The effect of grain size in NaCl powder samples and the effect of the purity of the materials used on their behavior during thermal treatment were determined. Experiments were carried out on samples with undefined size (raw NaCl), particle sizes of 100 and 200 μ m (sieved raw NaCl), different moisture levels, and different purity (NaCl purified by zone refining). The thermomechanical analysis (TMA) showed that reducing the grain size led to earlier grain densification and subsequent sintration as well as the influence of the purity. XRPD analysis was used to determine the structure and phase composition, confirming the presence of only NaCl. On the contrary, the MS proved the presence of a small content of H_2O , which was released at temperatures similar to those at the ND's rounding occurred, indicating a possible contribution of water in the NaCl catalytic action on NDs.

Author Index

Gregor Tomáš, 30

Α Guguschev Christo, 56 Abas Marcel, 15 Gushchina Liudmila, 67 Allix Mathieu, 64 Η В Halmanová Michaela, 18, 19 Babalová Eva, 16, 17 Hanada Takashi, 33, 49, 61 Babin Vladimir, 40, 64 Hanus Michal, 35 Babin Vladimír, 56 Hausnerová Berenika, 22 Bárta Jan, 26 Havlák Lubomír, 26, 39 Bartík David, 35 Havlíček Jan, 52 Bartosiewicz Karol, 34, 67 Hebnár Michal, 57 Behúlová Mária, 16, 17, 36 Holovský Jakub, 53 Bílek Ondřej, 35 Horiai Takahiko, 67 Blinová Lenka, 21 Hostinský Tomáš, 24, 37 Boháček Pavel, 39 Hrabovský Jan, 63 Buryi Maksym, 51, 59 Hrnčířová Vendula, 54 Bystřický Aleš, 70 Hsu Hua S., 53 Hudecová Silvia, 25, 62 \mathbf{C} Černičková Ivona, 18, 19, 21 Ι Cesnek Martin, 41 Illichmanová Edita, 25, 62 Chaika Mykhailo, 30 Ishizawa Satoshi, 33, 49, 61 Chvalníková Veronika, 25, 62 Čička Roman, 18, 46 Jain Naini, 53 D Jakeš Vít, 56 Damazyan Grigori, 30 Jarý Vítězslav, 26, 56, 64 Danišovičová Patrícia, 18, 19 Jelínková Helena, 39, 52, 55 Dobrovodský Jozef, 69 Ježek Jakub, 26, 27 Drienovský Marián, 18, 19, 21 Jorík Vladimír, 28 Ďuriš Rastislav, 20 Jurek Karel, 39 Ďuriška Libor, 18, 19, 21 Jurina František, 29, 65 \mathbf{E} K Endlerová Dagmar, 22, 42 Kadlec Kryštof, 55 Kajan Juraj, 30 F Kamada Kei, 31, 33, 49, 61, 67 Fabušová Diana, 23 Kamenský Miroslav, 32 Falvey Alexandra, 70 Kamrádek Michal, 63 Ferenčík Filip, 23 Kawabata Ryosuke, 33 G Kim Kyoung J., 61 Galusek Dušan, 30 Kim Kyoung Jin, 33, 49, 67

Kindl Herbert, 34, 56

Knedlová Jana, 35, 42 Kotian Martin, 36 Kotianová Janette, 36 Koudelka Ladislav, 24, 37 Kovačócy Pavel, 48 Kožíšek Zdeněk, 38 Král Robert, 26, 38, 40, 70 Kratochvíl Jan, 39, 52 Křehlíková Kateřina, 40 Kryštůfek Robin, 63 Kubiš Matej, 41 Kubišová Milena, 42 Kučerková Romana, 40, 56 Kucmanová Alexandra, 43, 57, 58 Kudo Tetsuo, 49 Kuliček Jaroslav, 53 Kurosawa Shunsuke, 33, 61 Kurosawa Syunsuke, 49 Kusý Martin, 21 Kutsuzawa Naoko, 33

\mathbf{L}

Labaš Vladimír, 44 Labašová Eva, 44 Lee Ya-Ju, 66 Lenghart Samuel, 50 Liao Yen-Fa, 45 Lubdrovcová Barbora, 42

M

Machajdíková Tereza, 46 Machajdíková Terézia, 18 Markovičová Lenka, 47, 68 Martinkovič Maroš, 48 Mašláni Alan, 51 Michalík Jakub, 30 Mošner Petr, 24, 37 Mukherjee Santanu, 21 Murakami Rikito, 33, 49, 61 Murugesan Naveenkarthik, 49

\mathbf{N}

Nakanishi Kohei, 67 Nakata Yuhei, 49 Nejezchleb Karel, 55 Nekvindová Pavla, 63, 64 Němec Michal, 39, 52 Neykova Neda, 53 Nikl Martin, 39, 40, 52 Noga Pavol, 23, 41, 69 Novák Martin, 22

O

Omuro Kazuya, 67

P

Palček Peter, 25, 62
Pata Vladimír , 22
Pätoprstý Boris, 29, 50
Pavlík Marián, 17
Pejchal Jan, 52, 56
Peterka Pavel, 63
Pilař Jakub, 51
Popelová Dominika, 39, 52
Prnová Anna , 30
Průša Petr, 40
Puchoňová Miroslava, 28

\mathbf{Q}

Qamar Muhammad, 54

\mathbf{R}

Rafajdus Jakub, 21 Reiter Jakub, 21 Remeš Zdeněk, 53 Rezek Bohuslav, 53, 54 Říha Adam, 55 Rohlíček Jan, 40 Rubešová Kateřina, 40, 56

S

Sahul Martin , 50 Sahul Miroslav, 17 Sato Hiroki, 33, 49, 61 Ščasná Margita, 43, 57, 58 Sedmidubský David, 27 Šenkeřík Vojtěch, 22 Ševeček Martin, 41 Sharma Rupendra K., 53 Sharma Shelja, 59 Šikyňa Lukáš, 25 Šimeková Beáta, 16, 48

Šimna Vladimír, 60

Simoniakin Artem, 63 Sirotiak Maroš, 43, 57, 58 Slezák Martin, 25, 62, 68 Soldán Maroš, 57, 58 Stehlík Štěpán, 70 Suezumi Hisato, 61 Šulc Jan, 39, 52, 55 Šurdová Zuzana, 25, 62 Švančárek Peter, 30 Száraz Zoltán, 69

\mathbf{T}

Thoř Tomáš, 56 Trunda Bohumil, 39

U

Uhríčik Milan, 25, 47, 62, 68 Ukraintsev Egor, 53, 54 Usuki Yasuyuki, 49

\mathbf{V}

Valová Tatiana, 58
Vaněček Vojtěch, 26, 40, 70
Vařák Petr, 63, 64
Véron Emmanuel, 64
Veselský Karel, 55
Vicen Martin, 68
Volf Jakub, 64
Vopát Tomáš, 29, 50, 65
Vozár Marek, 29, 65
Vretenár Viliam, 23
Vyhlídal David, 55

\mathbf{Y}

Yamaji Akihiro, 33, 49, 61 Yamamoto Seiichi, 67 Yao Yung-Chi, 66 Yokota Yuui, 33, 49, 61 Yoshikawa Akira, 33, 49, 61, 67 Yoshino Masao, 33, 49, 61, 67

\mathbf{Z}

Zajíc František, 34 Zajko Dominik, 29 Zatkalíková Viera, 47, 68 Zavadilová Pavlína, 69 Zemenová Petra, 38, 40, 70

LIST OF PARTICIPANTS

Marcel Abas (Slovak University of Technology in Bratislava, Trnava, 917 24, Slovakia)

Eva **B**abalová (*Slovak University of Technology in Bratislava*, 91724 Trnava, *Slovakia*) Mária Behúlová (*Slovak University of Technology in Bratislava*, 917 24 Trnava, *Slovakia*)

Ivona Černičková (*Slovak University of Technology in Bratislava*, 917 24 Trnava, *Slovakia*)

Patrícia **D**anišovičová (*Slovak University of Technology in Bratislava Faculty of Materials Science and T, Trnava, Slovakia*)

Rastislav Ďuriš (*Slovak University of Technology in Bratislava*, 917 24 Trnava, *Slovakia*) Libor Ďuriška (*Slovak University of Technology in Bratislava*, 917 24 Trnava, *Slovakia*)

Dagmar Endlerová (Tomas Bata University in Zlín, Faculty of technology, 760 01 Zlín, Czechia)

Filip **F**erenčík (*Slovak University of Technology in Bratislava*, 917 24 *Trnava*, *Slovakia*)

Tomáš **H**ostinský (*University of Pardubice*, 532 10 *Pardubice*, *Czechia*) Silvia Hudecová (*University of Žilina*, 010 26 Žilina, *Slovakia*)

Vitezslav **J**ary (Institute of Physics of the Czech Academy of Sciences, Prague 6, Czechia)

Jakub Ježek (Institute of Physics of the Czech Academy of Sciences, 182 00 Prague 8, Czechia)

Vladimír Jorík (Slovak University of Technology, Bratislava, Slovakia)

František Jurina (Slovak University of Technology in Bratislava, 917 24 Trnava, Slovakia)

Juraj **K**ajan (*University of Žilina*, 010 26 Žilina, *Slovakia*)

Kei Kamada (Tohoku University, Sendai, Japan)

Miroslav Kamenský (TESTOVACÍ TECHNIKA s.r.o., 290 01 Poděbrady, Czechia)

Ryosuke Kawabata (Tohoku University, 980-8577 Sendai, Japan)

Herbert Kindl (Institute of Physics of the Czech Academy of Sciences, Prague, 162 00, Czechia)

Jana Knedlová (Tomas Bata University in Zlín, 760 01 Zlín, Czechia)

Janette Kotianová (*Slovak University of Technology in Bratislava*, 917 24 Trnava, *Slovakia*)

Ladislav Koudelka (Univerzity of Pardubice, Pardubice, Czechia)

Zdeněk Kožíšek (Institute of Physics of the Czech Academy of Sciences, 162 00 Praha 6, Czechia)

Jan Kratochvíl (Czech Technical University in Prague, Prague, 115 19, Czechia)

Kateřina Křehlíková (Institute of Physics of the Czech Academy of Sciences, 162 00 Praha 6, Czechia)

Matej Kubiš (*Slovak University of Technology in Bratislava*, 917 24 Trnava, *Slovakia*)

Milena Kubišová (*Tomas Bata University in Zlín*, 760 01 Zlín, *Czechia*)

Alexandra Kucmanová (*Slovak University of Technology Bratislava*, 917 24 Trnava, *Slovakia*)

Eva Labašová (Slovak University of Technology in Bratislava, 917 24 Trnava, Slovakia)
Samuel Lenghart (Slovak University of Technology in Bratislava, 917 24 Trnava, Slovakia)
Yen-Fa Liao (National Synchrotron Radiation Research Center, 300092, Hsinchu, Taiwan)

Tereza **M**achajdíková (*Slovak University of Technology in Bratislava*, 917 24 Trnava, *Slovakia*) Lenka Markovičová (*University of Žilina*, 010 26 Žilina, *Slovakia*) Maroš Martinkovič (*Slovak University of Technology in Bratislava*, 917 24 Trnava, *Slovakia*)

Yuhei Nakata (*Graduation School of Engineering, Tohoku University, Sendai, 980-8579, Japan*)

Boris **P**ätoprstý (*Slovak University of Technology in Bratislava*, 917 24 Trnava, *Slovakia*)

Jakub Pilař (*Institute of Plasma Physics of Czech Academy of Sciences*, 182 00 Prague, *Czechia*)

Dominika Popelová (*Czech Technical University in Prague*, *FNSPE*, *Prague*, 12000, *Czechia*)

Zdeněk **R**emeš (*FZU* - Institute of Physics of the Czech Academy of Sciences, 182 00 Praha 8, Czechia)

Bohuslav Rezek (České vysoké učení technické v Praze, Praha 6, 166 27, Czechia)

Adam Říha (Czech Technical University in Prague, Praha, Czechia)

Kateřina Rubešová (University of Chemistry and Technology, Praha 6, Czechia)

Margita Ščasná (Slovak University of Technology in Bratislava, 917 24 Trnava, Slovakia)
Shelja Sharma (Institute of Plasma Physics, 182 00 Prague 8, Czechia)
Vladimír Šimna (Slovak University of Technology in Bratislava, 917 24 Trnava, Slovakia)
Hisato Suezumi (Graduation school of Engineering, Tohoku University, Miyagi, 984-0812, Japan)

Milan **U**hríčik (*University of Žilina*, 010 26 Žilina, *Slovakia*)

Petr Vařák (University of Chemistry and Technology, Prague, Praha 6, Czechia)

Jakub Volf (University of Chemistry and Technology Prague, 166 28, Prague, Czechia)

Marek Vozár (Slovak University of Technology in Bratislava, 917 24 Trnava, Slovakia)

Yung-Chi Yao (Program on Key Materials, National Cheng Kung University, 701, Taiwan) Masao Yoshino (Tohoku University, Sendai, Miyagi, 980-8577, Japan)

Dominik **Z**ajko (*Slovak University of Technology in Bratislava*, 917 24 Trnava, *Slovakia*)

Viera Zatkalíková (*University of Žilina*, 010 26 Žilina, Slovakia)

Pavlína Zavadilová (*Slovak University of Technology in Bratislava*, 917 24 Trnava, Slovakia)

Petra Zemenová (*Institute of Physics of the Czech Academy of Sciences*, *Prague 162 00*, *Czechia*)

teste

ModuLab XM MTS is configurable design for materials, electrochemistry and photovoltaic measurements in one chassis



